Assessing the hazard of saltwater intrusion in coastal regions of the Red-Thai Binh River Basin, Vietnam

Vu Thanh Tu[1,*], Nguyen Mai Dang[2], Nguyen Van Dao[3], Alexandre S. Gagnon[4]

[1] Water Resources Faculty, Thuyloi University, 175 Tay Son, Kim Lien, Hanoi 100000, Vietnam

[2] School of International Education, Thuyloi University, 175 Tay Son, Kim Lien, Hanoi 100000, Vietnam

[3] Center for Hydro - Meteorological Survey, Technology and Services, 10 Phao Dai Lang, Lang, Hanoi 100000, Vietnam

[4] School of Biological and Environmental Sciences, Liverpool John Moores University, Liverpool L3 3AF, United Kingdom

Abstract

The Red–Thai Binh River Basin in Vietnam faces severe saltwater intrusion, exacerbated by climate change, upstream water use, and inadequate reservoir management. During the dry season, reduced upstream discharge leads to higher salinity at sluice gates, thereby limiting the duration of the water supply. This study aims to assess and classify saltwater intrusion hazards in the basin under varying MIKE11 model upstream-flow and sea-level-rise scenarios. To achieve this, a multi-step framework was applied. First, the model was used to simulate saltwater intrusion dynamics, with calibration results showing strong performance (NSE = 0.72–0.92) and salinity deviations of less than 2.18‰. Second, simulated outputs were used to calculate average salinity at the commune level, enabling localised analysis. Third, a hazard classification system was developed by integrating average salinity levels with water-supply duration at sluice gates, thereby capturing both water-quality and availability constraints. The approach was applied to 15 scenarios across 243 coastal communes in the Nam Dinh and Thai Binh provinces, accounting for the combined effects of upstream discharge conditions and projected sea-level rise. The results reveal distinct spatial variations in saltwater intrusion hazards. In Nam Dinh Province, approximately 40–50% of communes were classified as having moderate-to-high hazard levels, indicating significant vulnerability. In contrast, in Thai Binh Province, most communes were classified below moderate hazard levels, suggesting comparatively lower risk. Overall, the findings identify priority areas where saltwater intrusion poses the greatest challenges and provide a basis for targeted adaptive management and improved water resource planning.

Keywords: saltwater intrusion, average salinity, water supply duration, hazard level mapping, Red-Thai Binh River Basin.

Highlight:

- Saltwater intrusion is increasingly intense and frequent in coastal regions due to climate change, rising sea levels, and upstream water resource use.
- This study proposed a method to evaluate and classify hazard levels based on average salinity and water supply duration.
- The study evaluated 15 scenarios accounting for the combined effects of upstream flow conditions and projected sea-level rise.
- The results reveal distinct spatial variations in saltwater intrusion hazards in Nam Dinh and Thai Binh Province, Vietnam.
- The findings highlight areas where saltwater intrusion poses the most significant challenges and where adaptive management measures should be prioritised.

Graphical Abstract

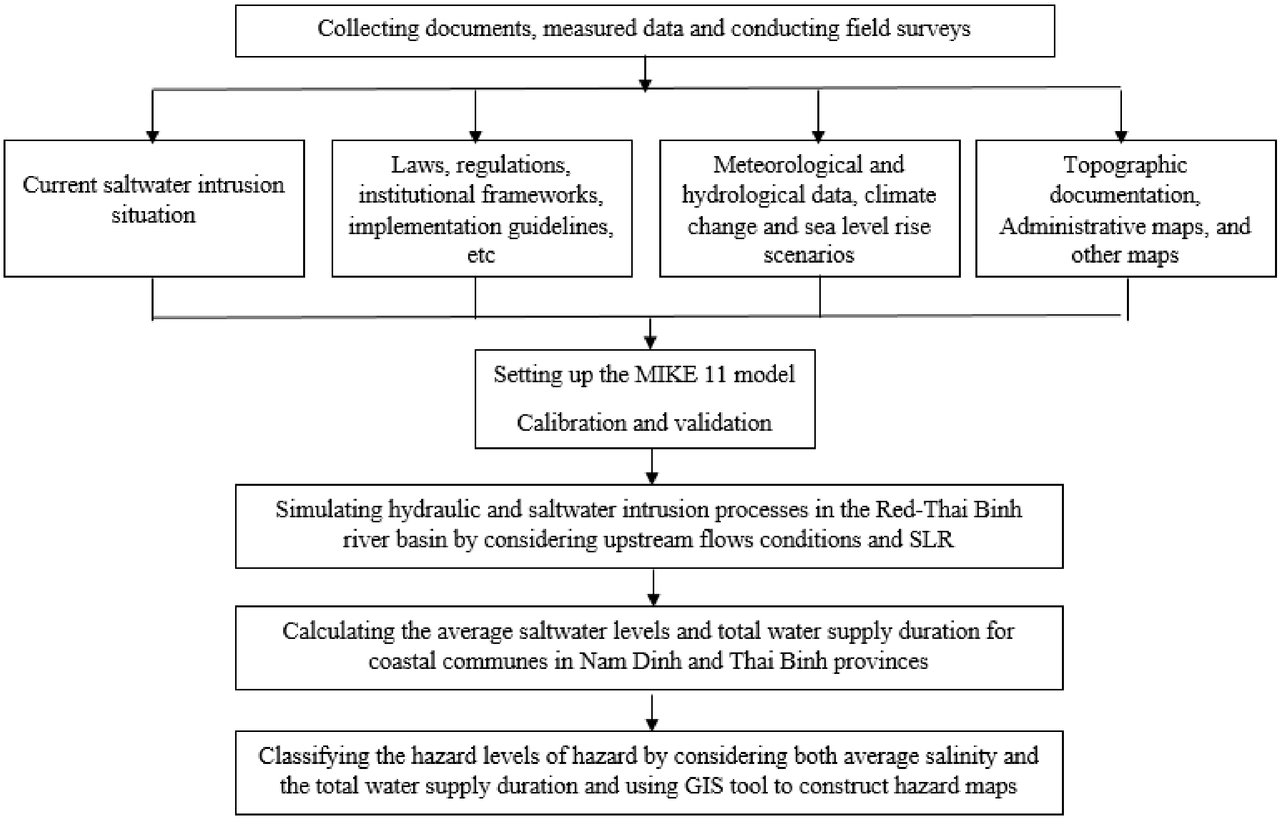

1. Introduction

Saltwater intrusion is a complex process occurring in coastal deltas and estuaries (Bear *et al.,* 1999), involving the replacement or mixing of freshwater with saltwater (Hebert, 2019). This phenomenon affects both surface water and groundwater systems (Tu *et al.,* 2021), and typically develops gradually over long periods. The interaction between hydrodynamic and human activities governs saltwater intrusion. Major controlling factors include upstream freshwater withdrawal, regulation of coastal flow, and Sea Level Rise (SLR) driven by climate change. (Liu *et al.,* 2019; Wang *et al.,* 2019; Zhang *et al.,* 2010). Tidal dynamics, storm surges, wind, wave action, estuarine geomorphology, and topography further influence the extent and variability of saltwater intrusion (Gong *et al.,* 2013; Liu *et al.,* 2017; Shen *et al.,* 2018; Perales-Valdivia *et al.,* 2018; Tian, 2019).

Recent advances in computational methods have enhanced the use of mathematical and machine learning models for analysing and predicting water quality dynamics (Maruthai *et al.,* 2025; Venkatraman *et al.,* 2025). Salinity is a key indicator for evaluating coastal hydrology and environmental conditions, particularly in the context of saltwater intrusion. To simulate saltwater intrusion processes, hydraulic interaction models of varying dimensionality have been developed, including one-dimensional (1D) (Lafta, 2022; Zhang *et al.,* 2013), two-dimensional (2D) (Haddout *et al.,* 2018; Lee *et al.,* 2016) and three-dimensional (3D) (Jeong *et al.,* 2010; Veerapaga *et al.,* 2019; Chen *et al.,* 2016) models. However, numerous studies have shown that the accuracy and reliability of complex models, such as 2D or 3D simulations, depend heavily on the availability of comprehensive observational datasets and, in many cases, require additional field surveys to ensure robust results (Kaddi *et al.,* 2022). Consequently, implementing such models in data-scarce regions remains a significant challenge (Lindenschmidt, 2006).

While higher-dimensional models offer detailed representations of hydrodynamic and solute transport processes, their computational demands often limit their practical application. To address these challenges, 1D models are frequently employed as efficient alternatives, incorporating simplifying assumptions to balance model complexity with predictive accuracy (Doulgeris *et al.,* 2012; Ferdous, 2014; Haque *et al.,* 2021; Miller, 2023; Vuong Tai *et al.,* 2021). When implemented with high temporal resolution, 1D models have demonstrated strong capability in reproducing the temporal dynamics of saltwater intrusion (Gaiolini *et al.,* 2023).

Simulation models have been widely employed to evaluate how flow regimes and tidal dynamics influence the spatial extent of saltwater intrusion (Becker *et al.,* 2010). In coastal estuaries, these processes are becoming increasingly complex due to the combined pressures of climate change and SLR (Bricheno et al., 2021; Ferguson & Gleeson, 2012; Hong et al., 2020; Oude Essink, 2001). This growing complexity poses substantial socio-economic risks for vulnerable regions (Khong et al., 2018; Meisner, 2007). A broad body of research further demonstrates that SLR plays a critical role in reshaping salinity regimes and contributing to the deterioration of coastal water quality (Erdbrügger et al., 2023; Rice et al., 2012; Thai & Thuc, 2011; Thanh et al., 2023; Yuan et al., 2015).

Vietnam has a coastline of over 3,200 km and is one of the countries most affected by natural disasters, including saltwater intrusion. In the context of climate change, saltwater intrusion is becoming more severe in the country (UNDP Vietnam, 2016). Recent studies have examined saltwater intrusion in Vietnam's large river basins, focusing on the impact of freshwater resources from upstream and SLR, notably in the Red-Thai Binh (RTB) River Basin (Hien *et al.,* 2018; Hien *et al.,* 2023). The RTB is an international river basin that flows through three countries: Vietnam, China, and Laos. It encompasses an area of approximately 169,000 km^2 (**Figure 1**). In Vietnam, the basin covers 86,680 km^2, accounting for 51.3% of the total area, with the delta region spanning approximately 17,000 km^2.

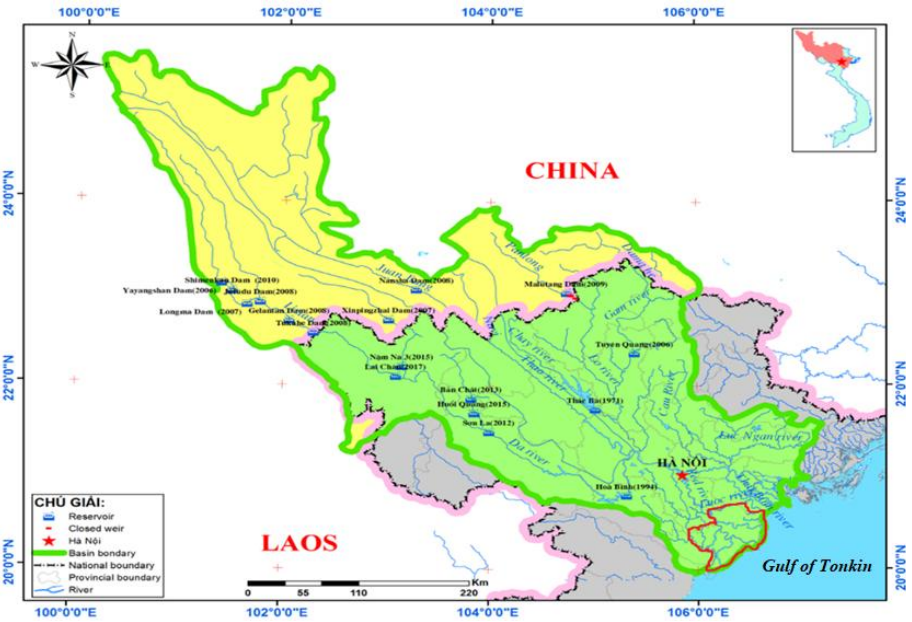

Figure 1. The RTB River basin in Vietnam (green area), and the boundary of Nam Dinh and Thai Binh provinces (red line).

The RTB River system discharges into the Gulf of Tonkin, located in the northwestern part of the South China Sea. The gulf is characterised by a diurnal tidal regime that produces some of the largest tidal amplitudes in Vietnam, reaching up to 4 metres. These tidal fluctuations have a strong influence on flow dynamics and saltwater intrusion processes across the eight estuaries of the RTB, particularly during the dry season from October to May, when river discharge is significantly reduced (Devienne, 2006).

The terrain of the RTB Delta is characterised by a gentle slope from northwest to southeast, with ground elevations ranging approximately from 0.4 to 9 meters above sea level (NARBO, 2006). This low-lying topography plays a crucial role in hydrodynamics, drainage patterns, and the delta's susceptibility to saltwater intrusion and flooding.

To supply water for agricultural activities, the rivers in the RTB Delta have about 432 sluices, whose operation depends on water demand, river level, and salinity. The system of sluices and canals creates a high-density water-supply network, ensuring water for communes and agricultural areas.

The salinity monitoring network in the RTB Delta comprises 18 stations, some of which have been active since 1963. However, these observations are not uniform; while some stations have recorded data for 15 to 20 years, others have only monitored salinity for 2 to 3 years. The data indicate that river salinity levels change seasonally. Salinity levels are low during the rainy season and high during the dry season, primarily influenced by the amount of freshwater released from upstream and the strength of tidal movements. The highest salinity levels are observed in January.

Many studies on saltwater intrusion in the RTB Delta have employed 1D models. A limitation of these studies is their focus on salinity processes in the main rivers only, while neglecting saltwater intrusion in the canal network. The findings indicate that saltwater can penetrate as far as 30 to 40 kilometres inland, with salinity levels exceeding 1‰ in some areas. Moreover, although salinity boundary maps have been created, they have been generated through linear interpolation of salinity levels along the main rivers, without considering the salinity in the internal canal network (Thai & Thuc, 2011). This methodology has its limitations and is open to varied interpretations. Additionally, limited research has examined the total duration of water supply from sluices, constraining a comprehensive assessment of saltwater intrusion impacts.

Previous investigations in the RTB Delta have been limited by the complexity of its river and canal networks and by the restricted spatial coverage of salinity monitoring stations. Furthermore, available salinity records are often discontinuous and lack temporal synchronisation among stations, hindering data interpretation and the construction of comprehensive salinity boundary maps. In most cases, salinity is measured at a single point along the river cross-section, which inadequately represents both horizontal and vertical variations in salinity distribution. To overcome these limitations, there is a need for more integrated and adaptive research approaches. For example, when evaluating the hazards posed by salinity, it is crucial to consider both average salinity concentrations and the duration of water availability. Hence, this study proposes a novel methodological framework for estimating average salinity levels in irrigated rice fields in deltaic and coastal regions. This framework is beneficial in situations where cross-sectional measurements are unavailable, and hydrodynamic models cannot effectively simulate salinity dynamics.

This study aims to develop a hazard map for saltwater intrusion based on average salinity levels and the total duration of water supply. The specific objectives are as follows: (1) to simulate the hydraulic and saltwater intrusion processes in the RTB River Basin during the peak dry season (January-March), considering the influence of upstream flow and SLR; (2) to calculate the average salinity levels and total water supply duration for 243 coastal communes in Nam Dinh and Thai Binh provinces that are most affected by saltwater intrusion in the RTB Delta; and (3) to create saltwater intrusion hazard maps that illustrate the impact levels on the communes under different SLR scenarios.

2. Methodology

Figure 2 illustrates the methodological approach used in this study.

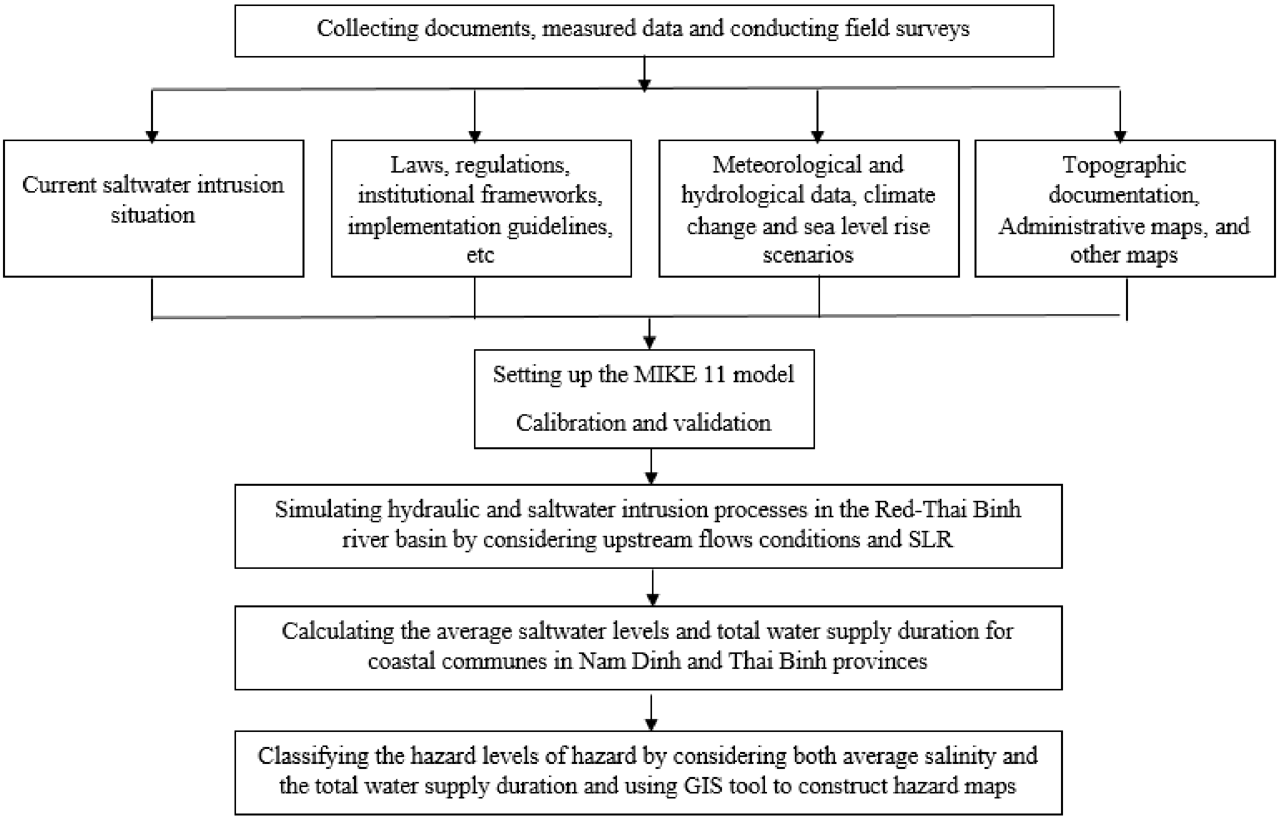

Figure 2. Flowchart of the research methodology.

2.1 Setting up the simulation model

1-D models utilised to simulate saltwater intrusion in river estuaries operate under the basic assumption that flow and salinity characteristics are uniform across the river's cross-section. Although this assumption may not be valid, the simulation results remain acceptable even with limited input data. Among the various 1-D models used to address this issue, the MIKE 11 model is particularly prominent. MIKE 11 simulates flow, sediment transport, and water quality in estuaries, rivers, irrigation systems, and canals. Additionally, it is recognised for its user-friendly dynamic modelling capabilities. Consequently, this study employed the MIKE 11 model to simulate saltwater intrusion in the RTB River Basin.

The model had nine upstream and eight downstream model boundaries (**Table 1**), with the latter located 15-25 km from the river mouth. The salinity at the upstream boundaries was set at 0‰, while the salinity at the offshore locations was 32‰, based on data recorded from 2000 to 2016 at Hon Dau station. For calibration and validation, this study used water-level, discharge, and salinity measurements from several downstream stations. **Figure 3** illustrates the river network, boundaries, and monitoring stations.

Table 1. List of upstream and downstream boundaries

No.	River	Station name	Location	
			LAT (°)	LONG (°)
Upstream boundaries				
1	Da	Hoa Binh	20.82	105.33
2	Thao	Yen Bai	21.70	104.86
3	Chay	Thac Ba	21.75	105.05
4	Lo	Ham Yen	22.05	105.09
5	Gam	Chiem Hoa	22.09	105.28
6	Cau	Gia Bay	21.60	105.83
7	Luc Nam	Chu	21.37	106.61
8	Thuong	Cau Son	21.45	106.32
9	Day	Ba Tha	19.92	105.58
Downstream boundaries				
1	Day		19.82	106.03
2	Ninh Co		19.89	106.25
3	Red		20.16	106.64
4	Tra Ly		20.44	106.70
5	Thai Binh		20.57	106.72
6	Van Uc		20.62	106.78
7	Lach Tray		20.76	106.84
8	Cam		20.77	106.88

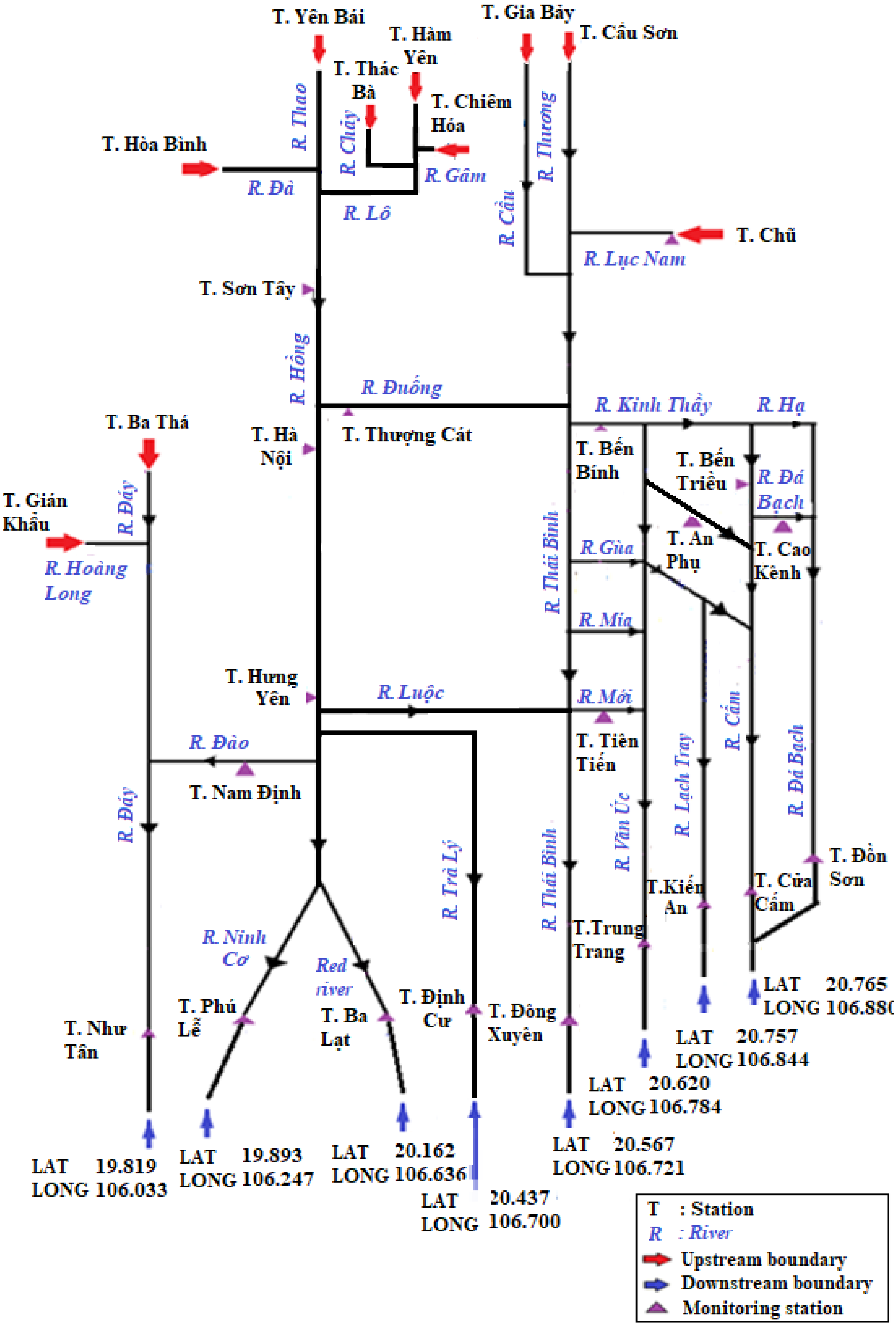

Figure 3. The modelled RTB River network.

The data used in this study reflect conditions from 2019 (**Table 2**). The modelled cross-section spans approximately 10 km in width and ranges in depth from 20 to 30 m, accurately representing the coastal topography. Simulations were run from January to March, during the peak of the dry season, characterised by minimal rainfall and lateral inflows. Initial conditions for flow discharge, water level, and salinity were based on field measurements to simulate intrusion processes and to calculate average salinity and water-supply duration, which were used to create hazard maps for affected coastal areas.

Table 2. The number of cross-sections on the simulation network's rivers

No.	**River**	**Number of cross-sections**	**No.**	**River**	**Number of cross-sections**
1	Cam	54	16	Lo	68
2	Cau	68	17	Luc Nam	23
3	Chay	50	18	Luoc	120
4	Da Bac	11	19	Mia	60
5	Dao	88	20	Moi	62
6	Day	78	21	Ninh Co	38
7	Duong	42	22	Pho Day	30
8	Gam	32	23	Quan Lieu	38
9	Hoa	48	24	Tam Bac	24
10	Hoang Long	18	25	Thai Binh	105
11	Red	63	26	Thao	78
12	Kinh Mon	80	27	Thuong	63
13	Kinh Thay	65	28	Tich	33
14	Lach Tray	75	29	Tra Ly	96
15	Lai Vu	57	30	Van Uc	53

The hydraulic (HD) and advection-dispersion (AD) modules in the MIKE 11 model were used together to simulate the salinity process. To calibrate and validate the parameter set, we followed a two-step trial-and-error method: (1) calibrating the HD parameter, specifically the Manning roughness coefficient (n), the Manning roughness coefficient is not fixed for the entire network but is zoned based on the morphological characteristics of each river section, and (2) calibrating the AD parameters, which include the dispersion factor (a), dispersion exponent (b), and dispersion coefficient (D), D is a function of velocity (u) as ($D = a \cdot |u|^b$). We evaluated the model's performance using the Nash-Sutcliffe Efficiency (NSE) coefficient and the absolute error (ΔS). The NSE and ΔS are calculated using **Equation 1** and **Equation 2**, respectively:

$$NSE = \frac{\sum_{i=1}^{n}(x_i - \bar{x})^2 - \sum_{i=1}^{n}(y_i - x_i)^2}{\sum_{i=1}^{n}(x_i - \bar{x})^2} \qquad (1)$$

$$\Delta S = |X_{max} - Y_{max}| \qquad (2)$$

where x_i and y_i are the measured and simulated values at each time i, $\bar{x}$ is the mean value of the measured time-series data; X_{max} and Y_{max} are the maximum measured and simulated values.

2.2 Development of salinity intrusion and climate change scenarios

To assess the influence of upstream flow and tidal levels on salinity, this study considered multiple scenarios: (1) three upstream flow conditions corresponding to the dry seasons of 2003, 1995 and 2015, which have return periods of approximately 20, 4 and 2 years, respectively, based on a frequency analysis of observed data from January to March for 1990-2020; and (2) tidal conditions represented by the 2011 tide level, used as an approximation of the average tide between 1990 and 2020 (scenario group A). In addition, SLR scenarios were examined for 2030, 2040, and 2050, under the RCP 4.5 pathway, and for 2050 under the RCP 8.5 pathway (scenario groups B-E). Combining upstream and downstream boundary conditions, a total of 15 simulation scenarios were considered (**Table 3**).

Table 3. List of simulated scenarios

No.	Scenario	Year of upstream discharge conditions	Downstream water level conditions for the year
1	1A		2011
2	1B		2030 RCP 4.5
3	1C	2003	2040 RCP 4.5
4	1D		2050 RCP 4.5
5	1E		2050 RCP 8.5
6	2A		2011
7	2B		2030 RCP 4.5
8	2C	1995	2040 RCP 4.5
9	2D		2050 RCP 4.5
10	2E		2050 RCP 8.5
11	3A		2011
12	3B		2030 RCP 4.5
13	3C	2015	2040 RCP 4.5
14	3D		2050 RCP 4.5
15	3E		2050 RCP 8.5

Figure 4 illustrates the discharge hydrograph, while **Figure 5** presents the average discharge and water levels recorded at various stations during the simulation period.

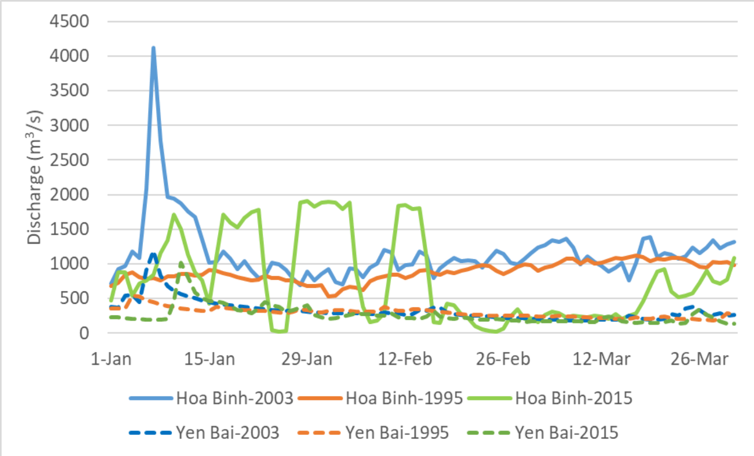

Figure 4. The discharge hydrograph from January 1 to March 31 of various years at selected stations.

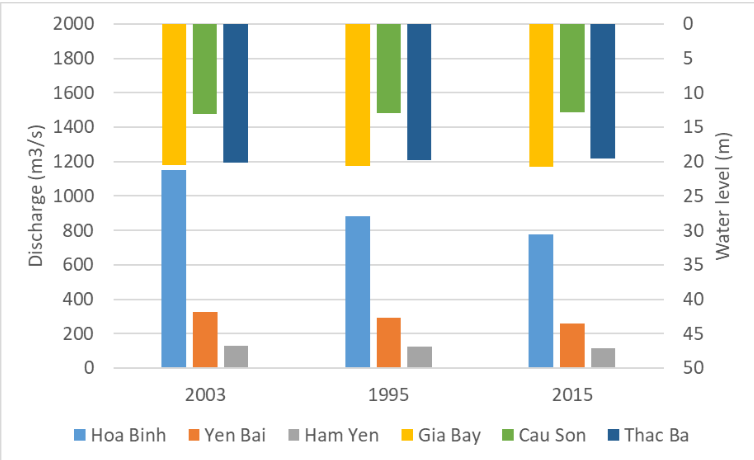

Figure 5. The average discharge and water level from January 1 to March 31 of various years at selected stations.

According to the national report on climate change and SLR scenarios released by the Ministry of Natural Resources and Environment of Vietnam (MONRE, 2021), sea levels are projected to rise by 12 cm, 17 cm, and 22 cm under the RCP4.5 scenario by the years 2030, 2040, and 2050, respectively. Additionally, a rise of 26 cm is expected by 2050 under the RCP8.5 scenario. This study calculated tide-level time series for sea level rise scenarios by averaging tide levels from 1990 to 2020 (using the 2011 water level value) and adding the projected increases for each corresponding year. We did not consider SLR in 2030 and 2040 under the RCP 8.5 scenario because the sea level difference between RCP 4.5 and RCP 8.5 in those decades is minimal. The time-series data of tide levels at the simulation network's downstream boundaries can be extracted from MIKE 21's Global Tide Model for 2011 (DHI, 2014). The data were adjusted to account for the time zone and altitude of the Vietnamese mainland (**Figure 6**).

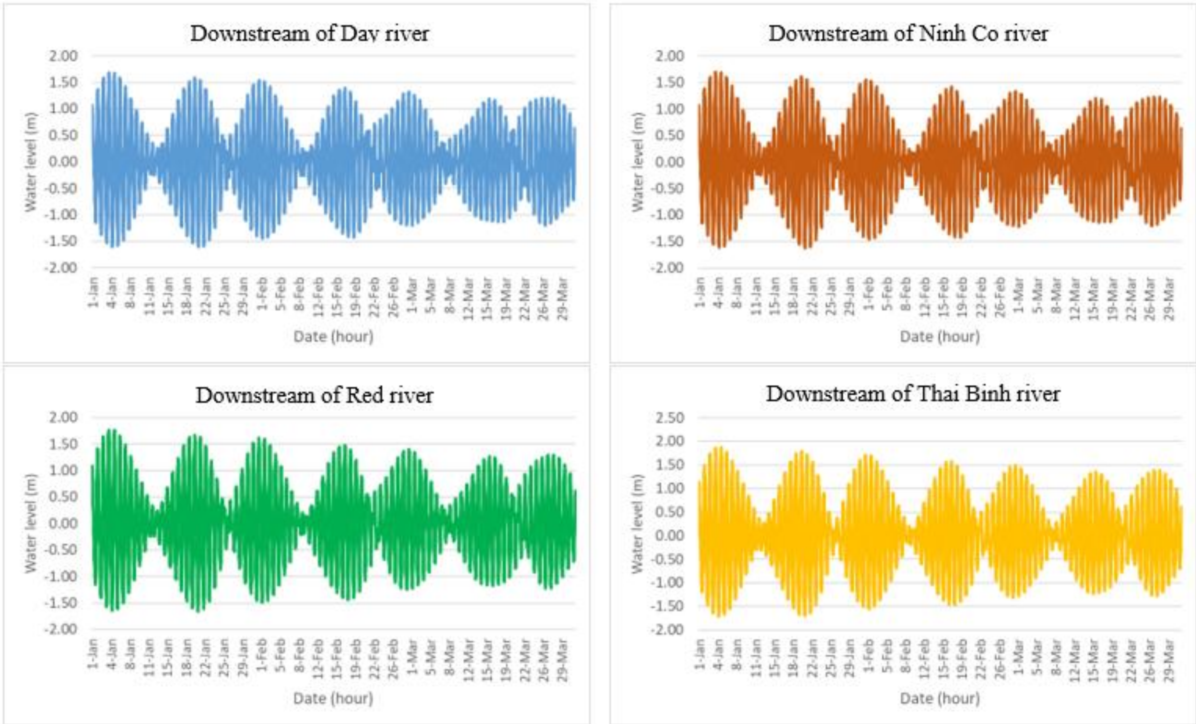

Figure 6. The tide level graph in 2011, as extracted from the MIKE model for different rivers

2.3 Assessing water supply duration and average salinity

The MIKE 11 model provides time-series data on water levels and salinity at specific locations and sluice gates along rivers for a given scenario. The total duration of water supply from each sluice across different scenarios k is determined based on two conditions: (1) the salinity in the main river for scenario (S_k) must be below the permitted level (S_p) for water to be supplied to the field, and (2) the water level in the river for scenario (Z_k) must be higher than the sluice bed elevation (Z_S). Thus, the total duration of the water supply for each sluice can be determined using this approach.

The spatial distribution of salinity in the study area is based on the following assumptions: (1) only saltwater intrusion through surface water systems is considered, excluding any intrusion into groundwater layers; (2) the salinity concentration within a commune is calculated based on the salinity levels measured at sluices, and (3) the dilution of water in canals and fields is not considered because the flows and salinity in those areas were not observed.

Based on the assumptions outlined above, as well as an analysis of salinity diffusion principles, mathematical logic, and the study area's conditions, this research proposes **Equation 3** to calculate the average salinity for a commune under various scenarios. The advantage of this formula is that it calculates the average salinity based on the ratio of the total water supply from each sluice. This method simplifies calculations and ensures reliable results.

$$S_{i,k} = \frac{\sum_{j=1}^{n}(V_{i,k,j} \ x \ S_{i,k,j})}{\sum_{j=1}^{n} V_{i,k,j}} \quad (3)$$

where $S_{i,k}$ is average salinity at a commune (i) corresponding to scenario (k), i ranges from 1 to 243 (total commune in the study area is 243), $V_{i,k,j}$ is total water supply (V_j) of the sluice (j) for a commune (i) corresponding to scenario (k), j ranges from 1 to n, n is the total number of sluice supply water for a commune (i), the total water supply of each sluice is determined based on its size (exploited discharge) and the supply duration corresponding to different scenarios. $S_{i,k,j}$ is the average salinity at the sluice (j) corresponding to scenario (k) supply water for a commune (i), see **Equation 4**.

$$\mathrm{S_{i,k,j}} = \frac{\sum_{\mathrm{t=1}}^{\mathrm{m}}(\mathrm{V_{i,k,j,t}} \ \mathrm{x} \ \mathrm{S_{i,k,j,t}})}{\sum_{\mathrm{t=1}}^{\mathrm{m}} \mathrm{V_{i,k,j,t}}} \quad (4)$$

where $S_{i,k,j,t}$ is salinity and $V_{i,k,j,t}$ is total water supply at the sluice (j) corresponding to scenario (k), supply water for a commune (i) has a salinity below the threshold in each supply duration (t), m denotes the total supply duration.

This example illustrates how to calculate the average salinity of commune X using **Equations 3** and **4**. The calculation involves taking water from the river to supply commune X through sluices A and B, as depicted in **Figure 7**.

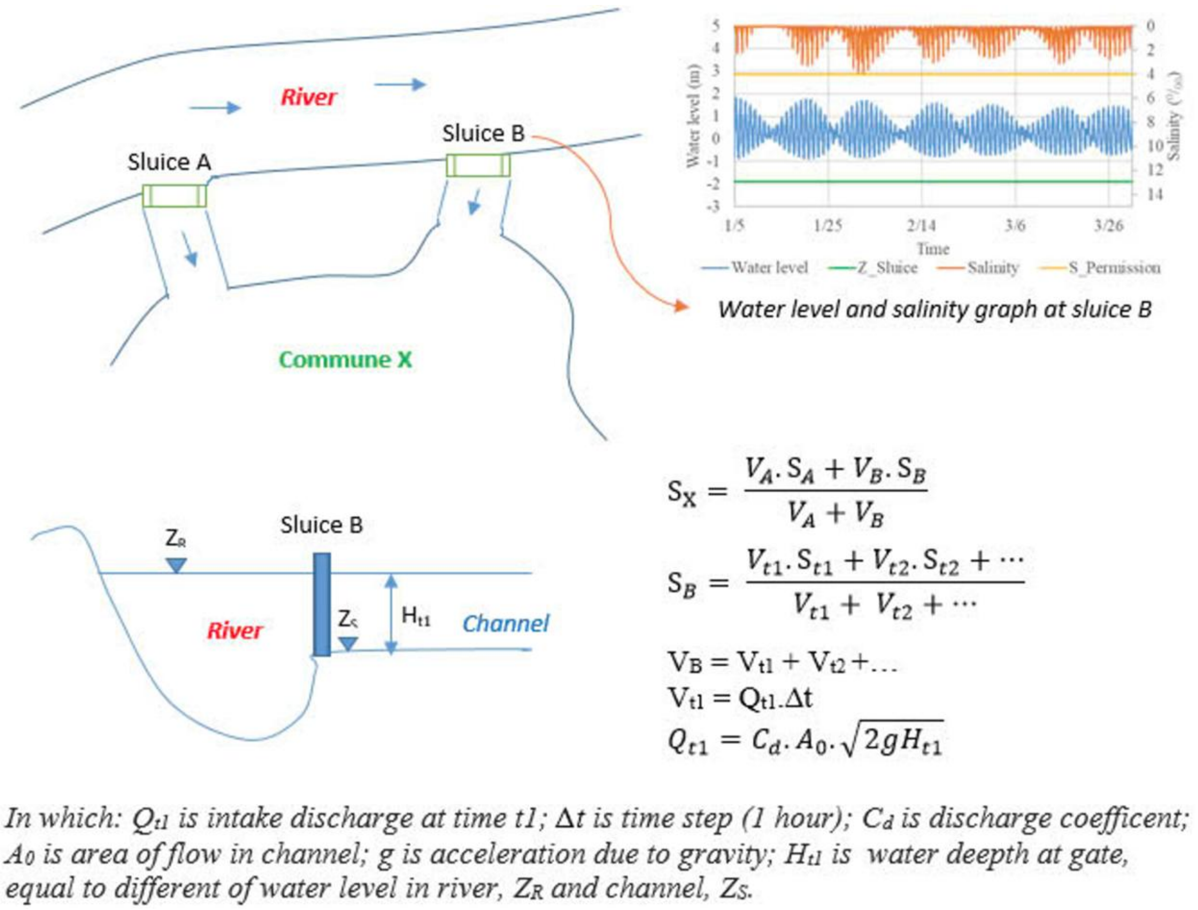

Figure 7. Diagram describing the method for calculating average salinity for a commune X according to **Equation 3** (as S_X) and **Equation 4** (as S_B).

2.4 Assessing salinity intrusion hazard

Following the IPCC (2014) and IPCC (2022), hazard is defined as the occurrence of a natural or man-made phenomenon, a physical impact, or a trend that is likely to cause loss of life, injury, or other health effects; as well as damage and loss to property, infrastructure, livelihoods, service provision, ecosystems, and environmental resources. Hazard level quantifies the intensity, magnitude, or probability of a particular hazard occurring at a specific location and time. Vulnerability is the tendency or inclination to be adversely affected. Vulnerability encompasses several concepts, including susceptibility to harm and a lack of capacity to cope and adapt. Risk is the potential for loss resulting from the dynamic interaction among the salinity hazard, exposure, and vulnerability. In this paper, hazard refers to the physical characteristics of salinity intrusion (concentration and duration) that pose a threat to the water supply. Hazard level is a quantified classification of the hazard's severity, categorised in this study into five levels (1–5) based on salinity thresholds and total water supply duration.

There are no specific regulations regarding the salinity threshold for water supply in Vietnam. However, to ensure safety, most Irrigation Operation Companies in the Nam Dinh and Thai Binh provinces only extract water from rivers when the salinity level is below 1‰.

Salinity levels between 1‰ and 4‰ may be suitable for specific crops (Kotuby-Amacher *et al.,* 2000). Therefore, to assess the hazards and impacts of saltwater intrusion in each commune within the study area, this study adopts a salinity threshold of 4‰. Still, with this threshold, the total duration of the water supply is limited. This results in significant water scarcity for agricultural activities in the affected area. From a hazard perspective, the total water supply duration is also important; a longer duration corresponds to a lower hazard level.

Researching on the effects of salinity on crops, Grismer & Bali, 2015; Kotuby-Amacher *et al.,* 2000) mentions a method for determining the crop yield reduction due to salinity as:

$$Y = 100 - B(ECe - A)$$

In which Y is the relative yield (%), A is the threshold value (dS/m), B is the percentage of yield reduction, and ECe is the average salinity in the field. The values of A and B are determined for different crop types.

In the study area, the salinity simulation period from January to March is when rice is primarily grown. Therefore, if the water is saline, crop yield may be reduced. According to Grieve et al. (2014), the coefficients A and B were determined to be 1.9 and 9.1 % per (dS/m), respectively. Therefore, given the yield reduction in rice plants under saline conditions, the study has classified the hazard levels associated with average salinity (H_S) into five distinct categories, as shown in **Table 4**.

Table 4. The hazard levels due to average salinity - H_S

Average salinity (‰)	Yield reduction (%)	Hazard level – H_S	Notes
≤ 1	0	0	No hazard
1.01 - 1.50	< 4	1	Very low
1.51 - 2.00	4.1÷11.1	2	Low
2.01 - 2.50	11.2÷18.3	3	Medium
2.51 - 3.20	18.4÷28.2	4	High
3.21 - 4.00	28.3÷39.6	5	Very high

Considering the total water supply duration, the simulation period from January 1 to March 31 was determined to be 2163 hours. This is also the dry season in the study area; therefore, the water supply for water management activities depends mainly on river water. In this study, we assumed that the sluice gate is fully opened when salinity and water level conditions permit. It can be seen that the total amount of water extracted through the sluice gate depends on the sluice gate size and the total supply duration. Therefore, the thresholds in Table 5 are calculated assuming that if the total supply duration exceeds 2051 hours, it meets over 95% of the water needs, which can be considered a no-hazard case. Conversely, if the total supply duration is less than 431 hours, it only meets about 20% of the water needs. Therefore, the hazard levels associated with the total water supply duration (H_T) have been classified into five distinct levels, as shown in **Table 5**.

Table 5. The hazard levels due to total water supply duration - H_T

Total supply duration (hours)	**Water demand (%)**	**Hazard level - H_T**	**Notes**

≥ 2051	95	0	No hazard
1728 - 2050	80÷94.9	1	Very low
1296 – 1727	60÷79.9	2	Low
864 – 1296	40÷59.9	3	Medium
432 – 863	20÷39.9	4	High
≤ 431	19.9	5	Very high

Equation 5 evaluates the hazard level at commune (i) for scenario (k) by considering the combined effects of average salinity and total water-supply duration.

$$H_{i,k} = w_S . H_{S_{i,k}} + w_T . H_{T_{i,k}} \qquad (1)$$

where $H_{i,k}$ is combined hazard level at a commune (i) corresponding to scenario (k), $H_{Si,k}$ is hazard level due to the average salinity at a commune (i) corresponding to scenario (k), $H_{Ti,k}$ is hazard level due to the total supply water duration at a commune (i) corresponding to scenario (k), w_S and w_T is the weighting factor of the hazard due to average salinity and total water supply duration, $w_S + w_T = 1$.

When salinity levels fall below the allowable threshold, the duration of the water supply becomes a critical factor because it directly determines the total volume delivered. For instance, if two drainage points of equal capacity extract water only when the salinity is below 4‰, the point with a longer extraction period will achieve a greater total intake. In this study, the weighting factors in Equation 5 were set at 0.4 for average salinity and 0.6 for total supply duration. The weighting factors were determined using the Analytic Hierarchy Process (AHP). Based on consultation with experts and local water management officials, the results showed that the importance of total supply water duration is approximately 1.5 times that of average salinity. Therefore, these values were chosen to reflect the greater practical importance of maintaining an adequate water supply over time, while still accounting for salinity in water quality. In other words, while salinity determines whether water is usable, the cumulative supply duration governs how much water can be effectively delivered to meet irrigation and domestic needs. The resulting hazard assessments under this weighting scheme are summarised in Table 6, with the corresponding hazard levels presented in Table 7.

Table 6. Combined hazard (H) of average salinity hazard (H_S) and total supply water duration hazard (H_T)

H		**H_T**					
		0	1	2	3	4	5
H_S	0	0	0.6	1.2	1.8	2.4	3.0
	1	0.4	1.0	1.6	2.2	2.8	3.4
	2	0.8	1.4	2.0	2.6	3.2	3.8
	3	1.2	1.8	2.4	3.0	3.6	4.2
	4	1.6	2.2	2.8	3.4	4.0	4.6
	5	2.0	2.6	3.2	3.8	4.4	5.0

Table 7. The classification of the combined hazard (H)

Hazard levels	**Combined hazard**	**Category**
1	< 1.50	Very low
2	1.50 – 2.50	Low
3	2.51 – 3.50	Medium
4	3.51 – 4.50	High
5	> 4.50	Very high

To create a saltwater intrusion hazard map for the study area, we first assessed the hazard value for each commune. Because of the complexity of the canal network, accurately determining the salinity spread within specific hazard zones is difficult. Therefore, we used administrative boundaries to delineate these areas.

3. Results and discussion

3.1 Calibration and validation of the simulation model

The calibration and verification results of the simulation model are presented in **Table 8**. The calibration of model parameters was conducted using data from January 1 to March 31, 2012. The findings show that the highest NSE coefficient, 0.92, was observed at the Son Tay station, where discharge measurements were taken. In contrast, the lowest NSE coefficient, 0.72, was recorded at the Truc Phuong water-level station. Calibrating parameters, such as roughness, in areas affected by tides poses significant challenges, often resulting in lower NSE coefficients. For example, the stations Truc Phuong, Quyet Chien, Cat Khe, Pha Lai, Quang Phuc, and Ben Trieu show less favourable results. In contrast, upstream areas that are not influenced by tidal effects yield better calibration results and higher NSE values. Successful stations in these upstream regions include Son Tay, Hanoi, Thuong Cat, and Hung Yen. Although some stations located in coastal estuaries exhibit poorer results, these outcomes still fall within an acceptable range.

The validation was conducted from January 1 to March 31, 2011. The model validation results show a pattern like that observed during model calibration. Specifically, the validation results for hydrological stations in the upper region, which is not affected by tides, show higher NSE coefficients than those from coastal plain stations that are significantly influenced by tides. As indicated in **Table 8**, the NSE efficiency coefficients for the Son Tay, Hanoi, Thuong Cat, and Hung Yen stations are all higher than those of the other stations, where the tidal process has a more substantial impact on the hydrological regime. This difference can be attributed to the greater complexity of hydrological processes (water levels and flows) in the tidal-influence area compared to the upstream region. In coastal areas, flow processes are governed by upstream flow and tidal influences at river mouths. Furthermore, as mentioned above, due to limitations in upstream input data, such as daily discharge, which lack sufficient smoothness compared to the hourly fluctuations in downstream tidal water levels, discrepancies may occur between calculated and measured values at high/low tides. In addition, the limited availability of riverbed topography data, which is subject to continuous sedimentation and erosion, also contributes to this problem. This dual influence leads to irregular, unpredictable fluctuations, making the model's calibration and verification more challenging and resulting in lower NSE values at some stations, such as Quyet Chien, which achieves only around 0.70.

Table 8. The NSE coefficient during the calibration and validation of the HD model

No	**Hydrological station**	**Measurement factor**	**NSE**	
			Calibration	Validation
1	Truc Phuong	Water level	0.72	0.72
2	Quyet Chien	Water level	0.88	0.70
3	Cat Khe	Water level	0.77	0.75
4	Pha Lai	Water level	0.80	0.78
5	Son Tay	Discharge	0.92	0.90
6	Hanoi	Discharge	0.92	0.90
7	Thuong Cat	Water level	0.88	0.87
8	Hung Yen	Water level	0.95	0.85
9	Quang Phục	Water level	0.81	0.81
10	Ben Trieu	Water level	0.82	0.82

Salinity observations at the monitoring stations are not recorded continuously but are instead limited to measurements taken during high and low tides each month. This intermittent sampling presents challenges for model calibration and validation. To address these limitations, the study assessed the performance of the AD model parameters using a restricted dataset and evaluated accuracy through the absolute error (ΔS) indicator. The difference between the maximum measured and simulated salinity values ranges from 0 to 2.18‰. Most stations exhibit a difference of less than 0.5‰ in the calibration (**Table 9**) and validation steps (**Table 10**).

Table 9. Absolute errors associated with the calibration of the AD model parameters at selected monitoring stations

No.	**Monitoring station / Sluice**	**Smax (‰)**		**ΔS (‰)**
		Simulated	Measured	
1	Tai	16.57	16.26	0.02
2	Ngo Dong	21.32	21.70	0.38
3	Xe	8.82	11.00	2.18
4	Con Nhat	16.16	16.00	0.16
5	Duong Lieu	0.33	0.14	0.19
6	Phuc Khe	0.41	0.36	0.05
7	Kinh Khe	1.72	1.40	0.32
8	Tien Tien	0.63	0.70	0.07
9	Cao Kenh	0.63	0.30	0.33
10	An Phu	0.05	0.05	0.00

Table 10. Absolute errors associated with the validation of the AD model parameters at selected monitoring stations

No	Monitoring station / Sluice	Smax (‰)		ΔS (‰)
		Simulated	Measured	
1	Phu Le	24.5	25	0.5
2	Dong Quy	26	24	2.0
3	Trung Trang	1.1	1.03	0.07
4	Dong Xuyen	11.7	12.1	0.4
5	Cao Kenh	1.3	1.29	0.01
6	Ba Lat	27.5	29.5	2.0
7	Don Son	2.2	2.3	0.1

The calibration and validation results show good agreement between the measured and observed values of the HD and AD modules, with reasonable trends in peak timing and magnitude. Despite some limitations in the salinity data and the MIKE 11 model's simplified advection and dispersion, the model performs adequately for simulating various scenarios in the study area.

3.2 Results of the salinity intrusion simulation scenarios

Although the study simulated hydraulic and water-quality dynamics across the entire RTB river system, the subsequent analysis focuses specifically on the Day, Ninh Co, Red, Tra Ly, and Thai Binh rivers. These rivers are regulated by sluice systems that supply water to all coastal communes in Nam Dinh and Thai Binh provinces.

3.2.1 The process of saltwater intrusion along the rivers

(1) Variations in upstream flow (Scenario group A)

Generally, if the tide level remains constant, an increase in upstream flow leads to a decrease in the maximum downstream salinity (**Table 11**) and a reduction in saltwater intrusion inland (**Figure 8**).

Table 11. The maximum salinity at some sluices on the rivers

River	Sluice	Maximum salinity (‰)		
		Scenario 1A	Scenario 2A	Scenario 3A
Day	Quy Nhat	11.98	12.00	12.02
	Thuan Hau	8.32	8.36	8.39
	Dong Lieu	4.90	4.96	4.98
	Tam Toa	0.60	0.61	0.63
Red	Ngo Dong	4.10	4.24	4.95
	Mo Dao	3.77	4.01	4.28
	Co Le	2.80	2.98	3.56
Ninh Co	Muc I	12.12	12.17	12.19
	Muc II	8.42	8.45	8.47
Tra Ly	Thai Phuc	5.05	5.20	6.25
	Nam Cuong	0.04	0.04	0.05
Thai Binh	Van Am	1.15	1.16	1.30
	Thu Cuc	0.61	0.63	0.73

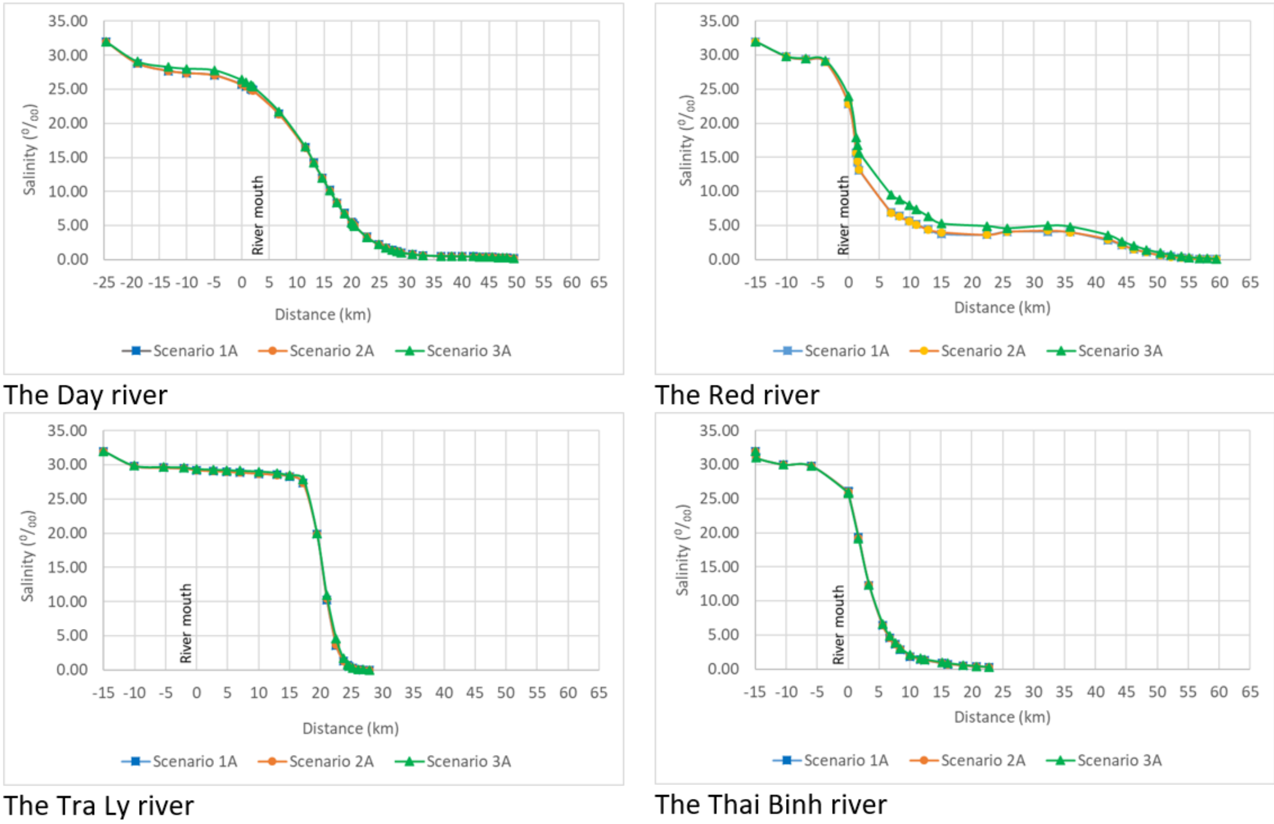

Figure 8. Salinity profiles of the studied rivers according to group A scenarios.

On the Day River, all simulation scenarios show similar trends in changes in maximum salinity along the river. Salinity decreases sharply from the river mouth toward the mainland. Specifically, between KM0 (the estuary) and KM22 (the mainland), salinity drops significantly from about 25‰ to less than 4‰. Beyond KM22, the maximum salinity along the river continues to decline steadily. The differences in maximum salinity along the river under different scenarios are relatively small, ranging from 0.2% to 5%. There is no significant reduction in the extent of saltwater intrusion into the mainland across the scenarios. In Scenario 3A, the distance from the river mouth to the point where salinity fell below 4‰ was 22 km, whereas in Scenario 1A it decreased slightly to 21 km. Likewise, the distance to where salinity falls below 1‰ decreased from 31 km in Scenario 3A to 29 km in Scenario 1A.

The Thinh Long Estuary on the Ninh Co River and the Ba Lat Estuary on the Red River are significantly affected by tidal influences. Additionally, the distribution of upstream flow from the Red River impacts salinity levels. As a result, most locations along the Ninh Co River experience maximum salinity levels exceeding 4‰ in all scenarios. However, the maximum salinity along the river quickly decreases from 26‰ (KM0) to 4‰ (KM45). The difference in maximum salinity at sluices between scenarios 1A, 2A, and 3A is minimal.

The Red River is the main river in the study region and has the strongest flow. Because of this, the highest salinity drops quickly from 23‰ at KM0 to about 5‰ at KM15. Comparing scenarios 1A and 2A, the change in maximum salinity at some locations is less than 6%, whereas between scenarios 1A and 3A, the change can be as significant as 40%. Comparing the results between scenarios 1A and 3A reveals a significant difference in the maximum salinity at several locations along the Red River. This phenomenon can be attributed to the non-linear interaction between upstream discharge and tidal energy. The Red River (main branch) has a higher discharge than other rivers regulated by upstream reservoirs. The small increase in discharge in scenario 1A compared to 3A creates a greater "pushing force" leading to lower salinity. Furthermore, the Red River's estuary has a more concentrated, deeper channel than the funnel-shaped estuaries of the Day River. When upstream flow increases, the velocity in the deep channel increases rapidly, directly neutralising the tidal energy entering the river. The distance from the river mouth to the position with salinity below 4‰ decreases from 37 km (scenario 3A) to 35 km (scenario 1A), and the position with salinity below 1‰ decreases from 50 km (scenario 3A) to 48 km (scenario 1A).

On the Tra Ly River, the salinity decreases slightly from the estuary up to around KM15, dropping from 29‰ to 28‰. However, between KM15 and KM22, the maximum salinity falls below 4‰. When comparing different scenarios, the maximum salinity levels indicate a slight decrease in the extent to which saltwater intrudes into areas. Specifically, the distance from the river mouth to locations with salinity below 4‰ decreases from 23 km (in scenario 3A) to 22 km (in scenario 1A). For locations with salinity below 1‰, it also decreases from 23 km (in scenario 3A) to 22 km (in scenario 1A).

The salinity of the Thai Binh River decreases significantly from the estuary to KM9, ranging from 26‰ to less than 3‰. The decrease is relatively steady upstream of the river. Across scenarios, the maximum salinity and the distance of saltwater intrusion remain relatively unchanged. The distance of saltwater intrusion decreases from 14 km (scenario 3A) to 12 km (scenario 1A).

The results indicate that salinity intrusion in the Day, Ninh Co, and Red rivers in Nam Dinh province is more severe than in the Tra Ly and Thai Binh rivers in Thai Binh province. This difference primarily stems from the distribution of water throughout the system during the dry season. The flow regulation from upstream to the Tra Ly and Thai Binh rivers is more abundant and stable compared to that of the Ninh Co and Day rivers, which have weaker and less stable flows.

Due to the stronger flow in Thai Binh province, rivers such as the Tra Ly create an effective "wall of fresh water" that helps prevent salinisation. Additionally, the riverbed terrain plays a role; for instance, the mouth of the Day River is wide and relatively shallow, allowing salinity to penetrate easily during high tides. In contrast, the Tra Ly river mouth is narrow and deep, with strong freshwater flow, which minimises salinity intrusion into this river.

This study evaluates the maximum salinity levels and the extent of river saltwater intrusion. It also determines the total duration of water supply at the sluices in the study area. The simulation period spans January to March, during which the total water supply duration could reach a maximum of 2,160 hours if salinity remains below the allowable threshold and the river level exceeds the sluice bed elevation. Generally, the total water supply duration at most sluices increases slightly between scenarios, ranging from 1 to 3 hours. However, at some sluices, such as the Muc I on the Ninh Co River, it experiences a more significant increase, rising from 70 to 93 hours (**Table 12**).

Table 12. Duration of total water supply at key sluices along the rivers

River	Sluice	Duration (hours) with salinity under 4‰		
		Scenario 1A	Scenario 2A	Scenario 3A
Day	Quy Nhat	1848	1837	1834
	Thuan Hau	1945	1930	1930
	Dong Lieu	1988	1986	1987
Red	Ngo Dong	1049	1046	1027
	Mo Dao	1997	1992	1984
Ninh Co	Muc I	716	646	623
	Muc II	1690	1658	1636

Our analysis of water supply duration across different salinity levels revealed varying changes. When salinity is below 1‰, the total water supply duration typically decreases due to lower upstream flow. For example, at the Mo Dao sluice, it drops from 1,728 hours in scenario 1A to 1,586 hours in scenario 3A. Conversely, when salinity is between 3.2 and 4‰, the duration increases, such as at the Quy Nhat sluice, where it rises from 34 to 43 hours, and at Muc II, from 83 to 119 hours.

Figure 9 shows how the total water supply duration varies across salinity levels under different scenarios.

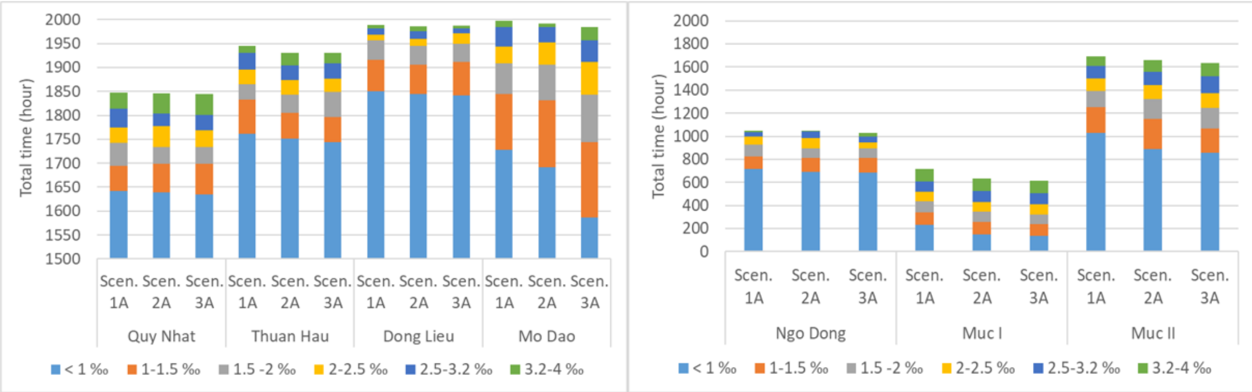

Figure 9. The total duration of water supply at various sluices for different salinity levels, according to different scenarios

(2) SLR scenarios

SLR is also a cause of salinity intrusion into rivers, along with upstream flow and topographic conditions. As SLR increases, both the maximum salinity at sluices and the extent of saltwater intrusion into the continent also rise (**Figure 10**). Furthermore, when there is reduced upstream flow coupled with elevated tide levels, the maximum salinity at the sluices increases, as illustrated in **Figure 11**.

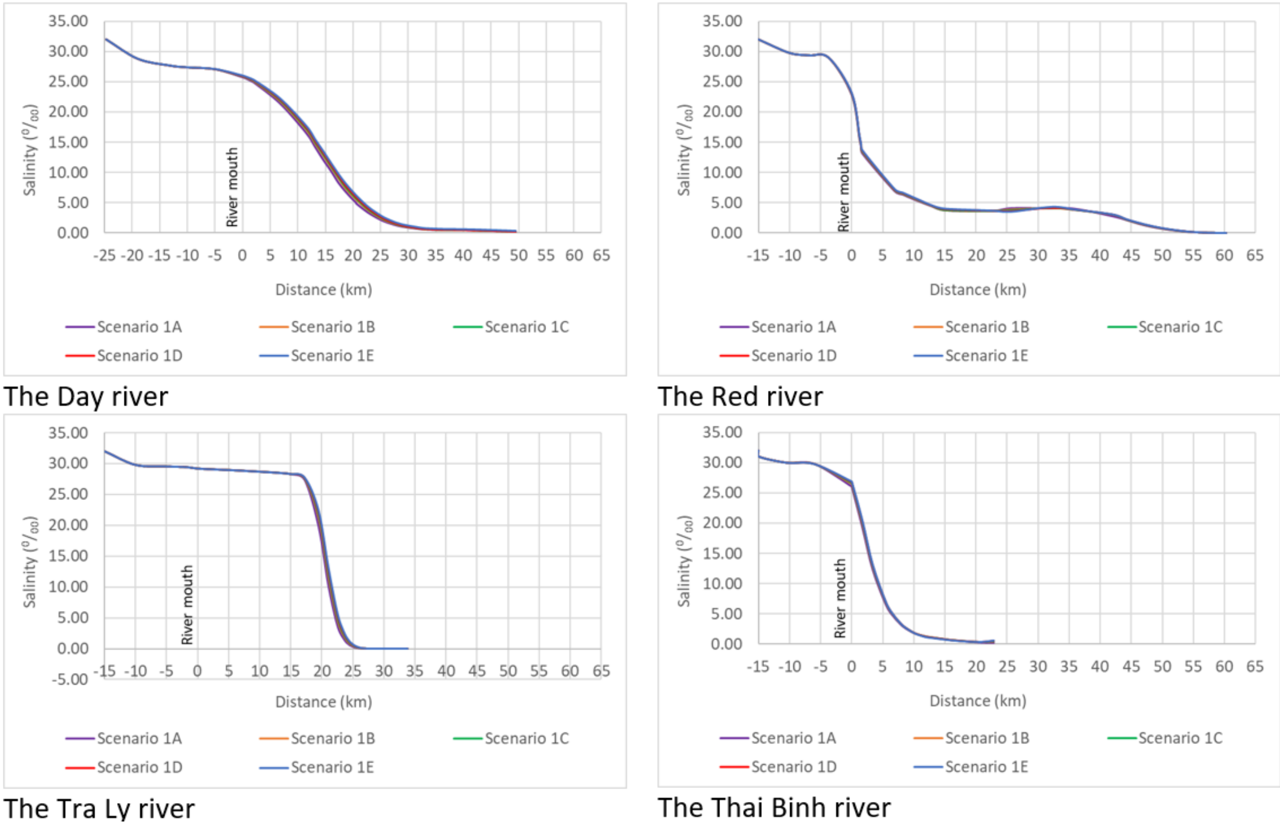

Figure 10. Salinity profiles of the studied rivers under different SLR scenarios.

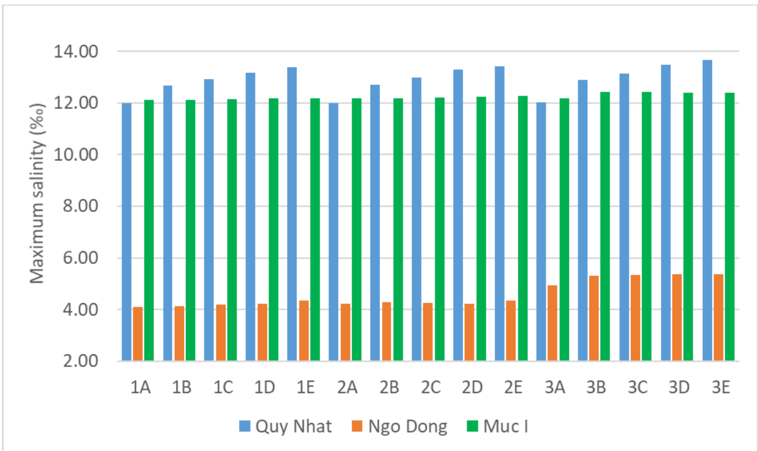

Figure 11. Maximum salinity at various sluice levels across different scenarios.

Compared to scenario group A, the maximum increase in salinity at the sluices on the Day River due to SLR is significantly greater, ranging from 6% to 39%. The saline increase on the Thai Binh River rose from 6% to 26%. Other rivers experienced much smaller increases, ranging from 1% to 10%. Additionally, the distance of saltwater intrusion into the land has increased by 1-2 kilometres. When salinity levels fall below the permitted threshold, the total duration of the water supply varies across different scenarios. For some sluices, such as Dong Lieu, Mo Dao, and Muc II, the decrease in supply is minimal, ranging from 1 to 8 hours. However, other sluices, such as Ngo Dong and Muc I, experience significant reductions, with decreases ranging from 32 to 305 hours (**Figure 12**).

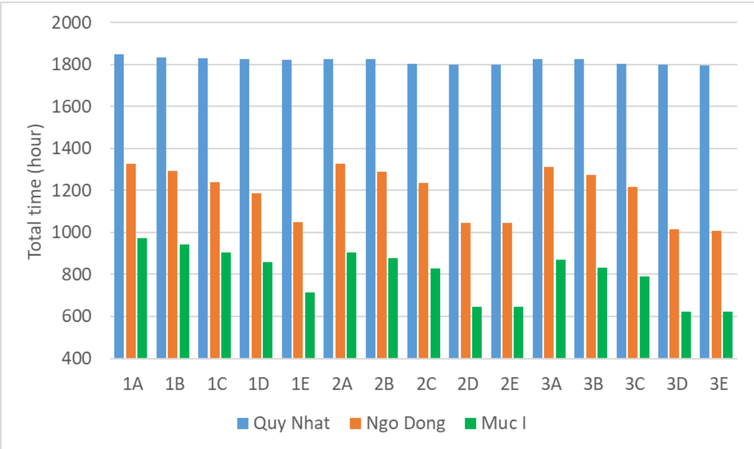

Figure 12. Total water-supply duration at various sluices across different scenarios.

3.2.2 The average salinity and hazard levels in communes

Figure 13 presents water-level and salinity measurements at various sluice gates throughout the simulation period across different scenarios. Using this data, we can calculate the average salinity for each commune by considering the total amount of water supplied from each sluice, as detailed in section 2.3.

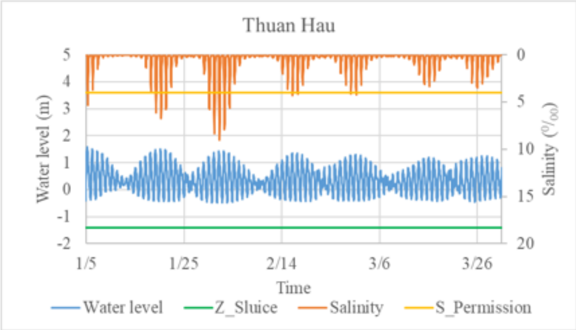

Thuan Hau sluice, Day River, scenario 1B.

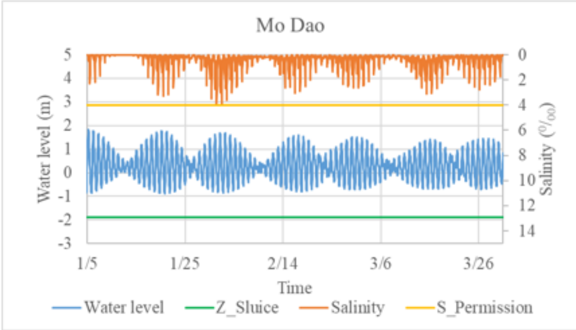

Mo Dao sluice, Red river, scenario 1C.

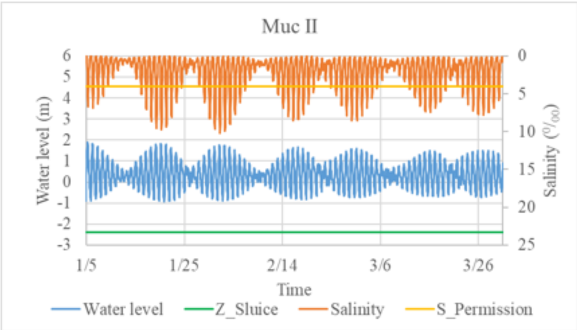

Muc II sluice, Ninh Co river, scenario 2D.

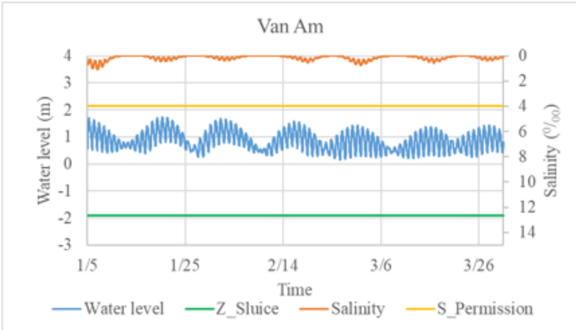

Van Am sluice, Thai Binh river, scenario 2E.

Figure 13. Water level and salinity graphs at selected sluices for various scenarios

An assessment of 123 communes in Nam Dinh province reveals that the number of communes exposed to salinity-related hazards has risen from 61 in scenario group 1 to 69 in scenario groups 2 and 3. Among these communes exposed to hazards at levels 1 to 3, the highest proportion, 60%, is at hazard level 2. A detailed analysis reveals that the number of communes at each hazard level varies with fluctuations in upstream flow and tide levels. For example, when comparing scenarios 1D, 2D, and 3D, the total number of communes exposed to hazard level 3 rises from 13 in scenario 1D to 28 in scenario 2D and 29 in scenario 3D (**Figure 14**).

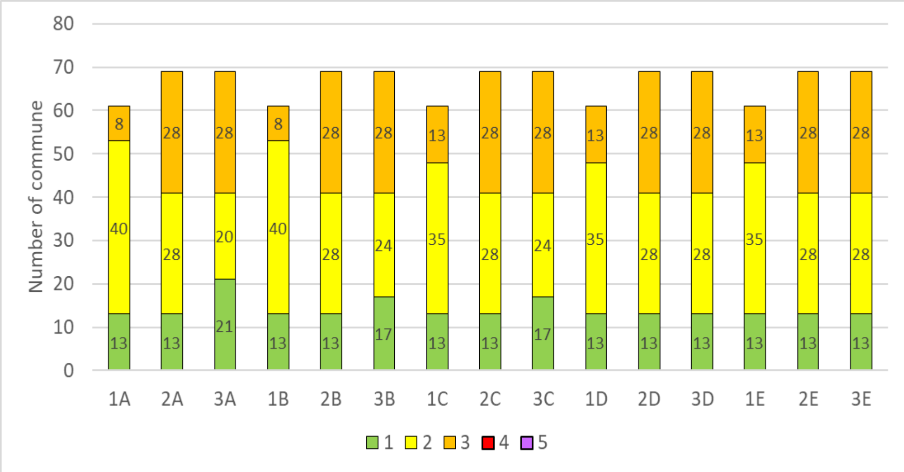

Figure 14. The total number of communes in Nam Dinh province affected by salinity hazards across various scenarios.

An assessment of 120 communes in Thai Binh province reveals that the total number of communes exposed to hazards due to the salinity factor is significantly lower than in Nam Dinh province. Only 16 to 21 communes, most at level 1, are exposed to hazards. Due to upstream flow and SLR, some communes changed from no hazard to level 1, while others changed from level 1 to level 2 (**Figure 15**). This is understandable because the salinity of the Thai Binh River is lower than that of other rivers, and there is no water supply issue if the salinity remains below the allowable threshold.

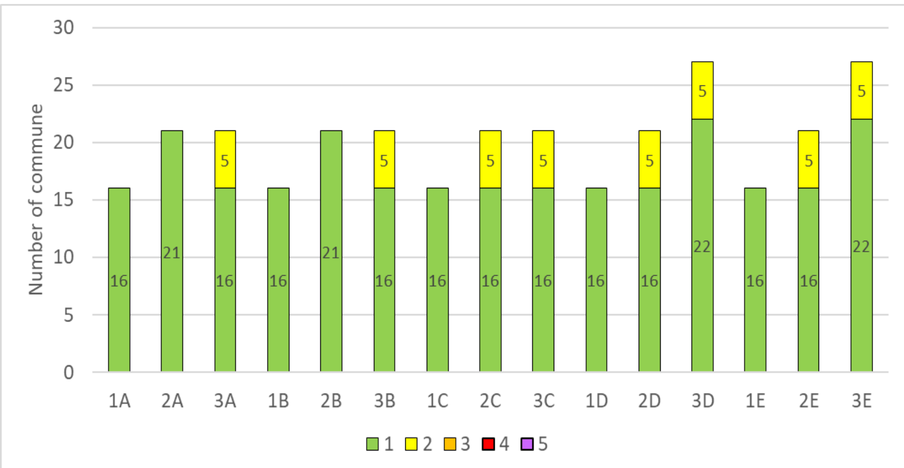

Figure 15. The number of communes in Thai Binh province facing various salinity hazard levels across scenarios.

Assessment of the hazard level due to water supply duration: all communes in Nam Dinh province are exposed to hazard levels of 1-5. The percentage of communes at level 3 is the highest, ranging from 30% to 56% across scenarios. Additionally, the number of communes at various levels increases as upstream flow decreases and sea levels rise (**Figure 16**).

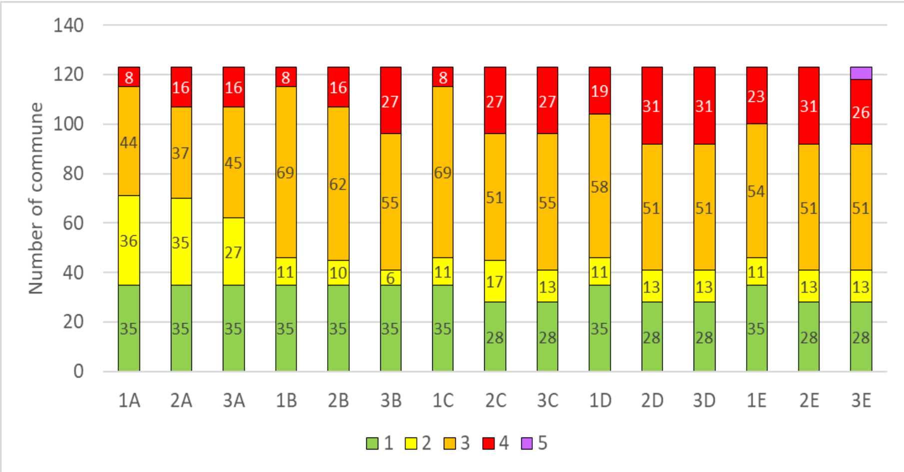

Figure 16. The number of communes in Nam Dinh province facing various hazard levels due to different water supply durations

Unlike Nam Dinh province, Thai Binh province's water supply duration is longer due to the lower impact of saline intrusion. All 120 communes in the study area are exposed to hazard levels ranging from 1 to 3, with 60% at level 1. While the number of communes at each level varies across scenarios, the change is minimal. Only three communes shift from levels 2 to 3 in scenario groups 2 and 3 (**Figure 17**).

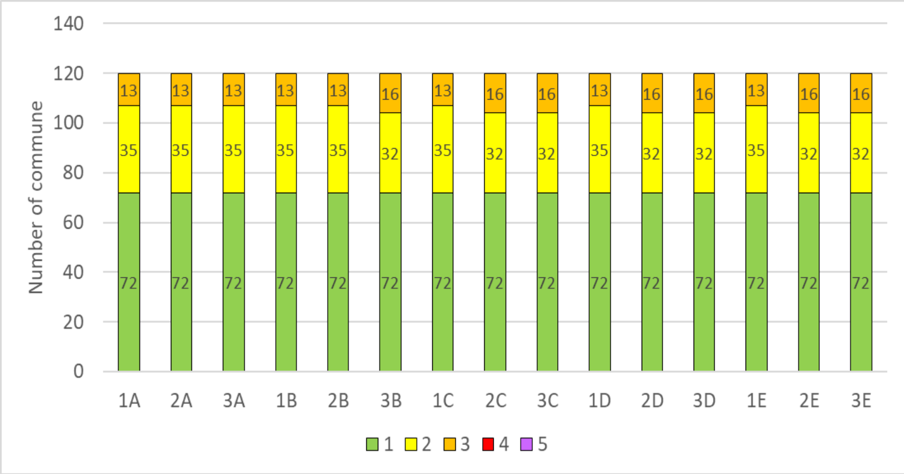

Figure 17. The total number of communes in Thai Binh province affected by varying hazard levels related to the duration of water supply

The interaction between salinity levels and water-supply duration can influence the hazard posed by saltwater intrusion. All communes in the study area of Nam Dinh province are exposed to hazard levels 1-4. The total number of communes at levels 2 and 3 accounts for approximately 40-60%, depending on the scenario. Due to reduced upstream flow, many communes have moved from low to higher hazard levels. For instance, between scenarios 1A, 2A, and 3A, seven communes have moved from level 1 to level 2, and 16 communes have moved from level 3 to level 4. Additionally, the number of communes vulnerable to high hazards has increased due to SLR. For example, between scenarios 1A and 1B, the number of communes exposed to hazard level 1 has decreased from 62 to 37, while the number of communes at hazard level 2 has increased from 13 to 38 (**Figure 18**). In this province, some communes identified as having the highest hazard levels are Hai Chau, Hai Hoa, Hai Ninh, Hai Trieu, and Thinh Long, all at level 4.

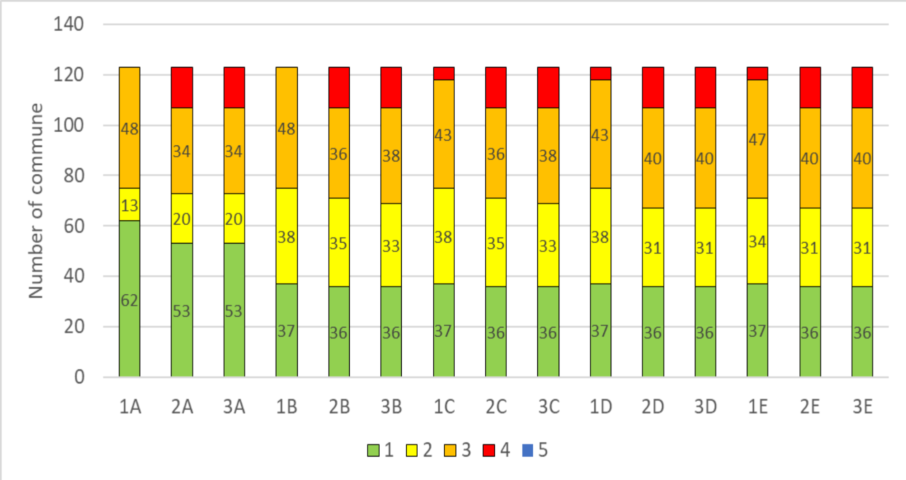

Figure 18. The total number of communes in Nam Dinh province exposed to different hazard levels under various scenarios

In Thai Binh province, all communes are only exposed to hazards at levels 1 and 2. Approximately 75% of them are exposed to level 1 hazards (**Figure 19**). The change in the number of communes exposed to hazards at different levels remains almost constant across scenarios. Some communes exposed to the highest hazard levels include Nam Chinh, Nam Hong, and Tay Phong, all of which are categorised as level 2.

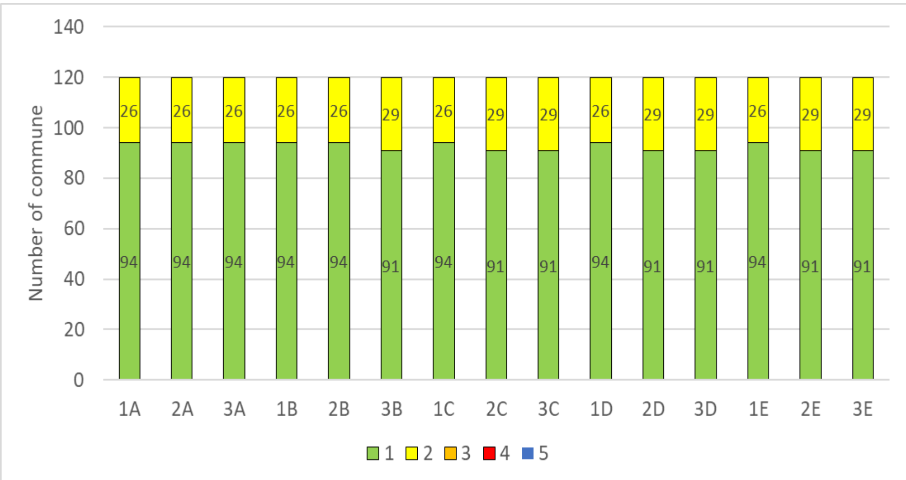

Figure 19. The number of communes in Thai Binh province exposed to various hazard levels under different scenarios

3.2.3 *Saltwater intrusion hazard maps*

Based on analyses of average salinity and water-supply duration, a saltwater intrusion hazard map was constructed for the 243 communes of the study area for the different scenarios. **Figure 20** shows the changes in hazard level across communes due to upstream flow conditions and SLR.

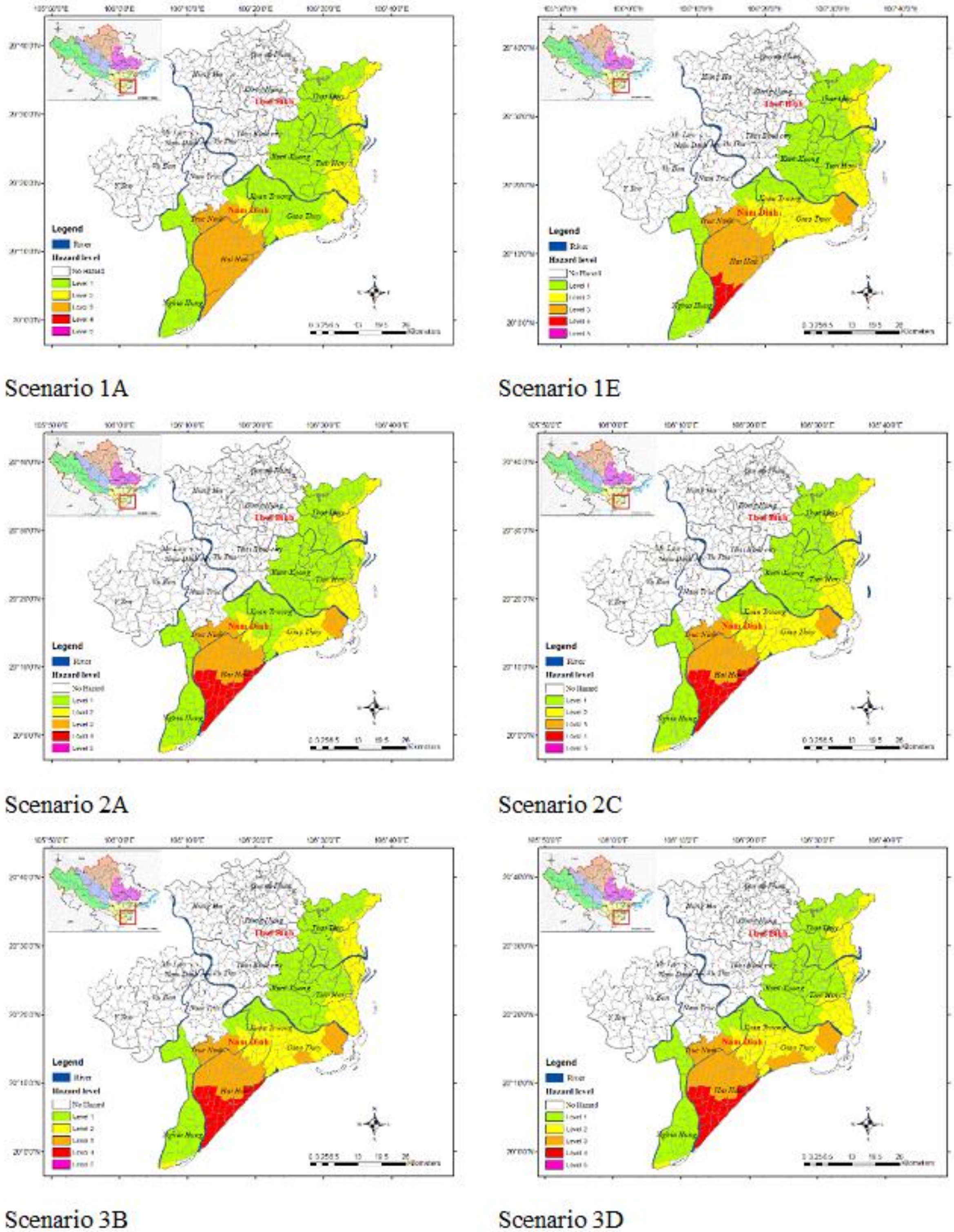

Figure 20. Saltwater intrusion hazard maps of the study area for different scenarios

Overall, communes in downstream areas are subject to greater saltwater intrusion hazards than those upstream. Districts such as Hai Hau, Giao Thuy, Tien Hai, and Thai Thuy face elevated risk because their water is drawn directly from river sluice gates, where salinity tends to be higher. In contrast, communes with well-developed canal networks and effective distribution of low-salinity water from upstream sources, such as those in the Nghia Hung district, exhibit comparatively lower hazard levels.

This study takes a more comprehensive approach to mapping salinity intrusion boundaries than previous research, which focused solely on the maximum simulated salinity along major rivers. Earlier methods often led to misrepresentations of salinity distribution in the RTB River Basin by neglecting inland variations and secondary channels. In contrast, the saltwater intrusion hazard map developed in this study offers a more accurate depiction of the spatial extent and intensity of the affected areas. This improved representation enhances our understanding of salinity dynamics. It allows for the identification of priority zones for management interventions, thereby supporting the development of targeted strategies to mitigate the impacts of saltwater intrusion.

4. Conclusions

Saltwater intrusion is a complex phenomenon influenced by factors such as upstream flow patterns, tidal dynamics, and other environmental conditions. Understanding how these elements interact is essential for assessing the impacts of saltwater encroachment in coastal and estuarine areas. This study used the MIKE 11 model to simulate saltwater intrusion in the RTB river basin by examining 15 scenarios that account for variations in upstream flow during the dry season and the effects of SLR. The findings suggest that maximum salinity levels in the river and the extent of saltwater intrusion are likely to increase due to reduced upstream flow and/or rising sea levels.

When analysing the impact of upstream flow changes on salinity levels at sluice gates, maximum salinity remains relatively stable across most rivers, with variations typically under 6%. However, the Red River shows more significant fluctuations, with salinity changes reaching up to 40%. In terms of SLR, both the Day River and the Thai Binh River experience more substantial salinity changes compared to other rivers. In all scenarios, saltwater intrusion extends 1 to 2 kilometres inland.

This paper presents a new approach to estimating the average salinity during the water supply period when salinity levels fall below the allowable threshold. The study determined the average salinity and the total duration of water supply for 123 coastal communes in Nam Dinh province and 120 in Thai Binh province. A comparison of results across scenarios reveals significant variations in average salinity and total water-supply duration, reflecting the different hazard levels experienced by each commune. All communes in Nam Dinh province face higher hazard levels compared to those in Thai Binh province. Specifically, the hazard levels in Thai Binh province range only from 1 to 2, while in Nam Dinh province, they range from 1 to 4.

Unlike previous studies that created saltwater intrusion boundary maps for the RTB River Basin, the hazard maps developed in this study provide a more accurate representation of the extent of saltwater intrusion and the associated hazard levels, despite some limitations in the available observational network. This improved precision is achieved by considering both the average salinity and the total duration of the water supply for the canal system. The findings of this study provide valuable insights for assessing risks for the development of adaptation strategies to mitigate the impacts of saltwater intrusion in the study region.

Further research is recommended in the following areas: (1) measuring cross-sections and salinity levels in the rivers and canals of the irrigation system. This data would be used to simulate hydrodynamics and salinity transmission throughout the entire system. Comparing these findings with the current results will provide a scientific basis for model calibration and validation, ensuring that the results align more closely with real-world conditions. (2) Investigating the operation of upstream reservoirs to enhance freshwater discharge, which could help reduce salinity levels during periods of strong tides in the downstream areas.

Acknowledgements

The authors thank the Vietnam Hydro-meteorological Data Center, Xuan Thuy, Nghia Hung, Nam Ninh, and Hai Hau Irrigation Operation Company in Nam Dinh Province, and Bac Thai Binh and Nam Thai Binh Irrigation Operation Company in Thai Binh Province, Vietnam, for their assistance with the collection of data required for this research.

References

Bear, J., Cheng, A., Sorek, S., Ouazar, D., & Herrera, I. (1999). *Seawater intrusion in coastal aquifers: concepts, methods, and practices*. https://api.semanticscholar.org/CorpusID:127213695

Becker, M. L., Luettich, R. A., & Mallin, M. A. (2010). Hydrodynamic behavior of the Cape Fear River and estuarine system: A synthesis and observational investigation of discharge-salinity intrusion relationships. *Estuarine, Coastal and Shelf Science*, *88*(3), 407–418. https://doi.org/10.1016/j.ecss.2010.04.022

Bricheno, L. M., Wolf, J., & Sun, Y. (2021). Saline intrusion in the Ganges-Brahmaputra-Meghna megadelta. *Estuarine, Coastal and Shelf Science*, *252*, 107246. https://doi.org/https://doi.org/10.1016/j.ecss.2021.107246

Chen, W., Chen, K., Kuang, C., Zhu, D. Z., He, L., Mao, X., Liang, H., & Song, H. (2016). Influence of sea level rise on saline water intrusion in the Yangtze River Estuary, China. *Applied Ocean Research*, *54*, 12–25. https://doi.org/10.1016/j.apor.2015.11.002

Devienne, S. (2006). Red River Delta: Fifty Years of Change. *Moussons*, *9–10*, 255–280.

https://doi.org/https://doi.org/10.4000/moussons.2042

DHI. (2014). *MIKE 21 Toolbox - Global Tide Model - Tidal prediction* (p. 20). DHI.

Doulgeris, C., Georgiou, P., Papadimos, D., & Papamichail, D. (2012). Ecosystem approach to water resources management using the MIKE 11 modeling system in the Strymonas River and Lake Kerkini. *Journal of Environmental Management*, *94*(1), 132–143. https://doi.org/https://doi.org/10.1016/j.jenvman.2011.06.023

Erdbrügger, J., van Meerveld, I., Seibert, J., & Bishop, K. (2023). Temporal and spatial variation in shallow groundwater gradients in a boreal headwater catchment. *Journal of Hydrology*, *626*(PB), 130301. https://doi.org/10.1016/j.jhydrol.2023.130301

Ferdous, A. (2014). Cumulative Hydrologic Impact of Wetland Loss: Numerical Modeling Study of the Rideau River Watershed, Canada. *Journal of Hydrologic Engineering*, *19*(3), 593–606. https://doi.org/10.1061/(ASCE)HE.1943-5584.0000817

Ferguson, G., & Gleeson, T. (2012). Vulnerability of coastal aquifers to groundwater use and climate change. *Nature Climate Change*, *2*(5), 342–345. https://doi.org/10.1038/nclimate1413

Gaiolini, M., Colombani, N., Mastrocicco, M., & Postacchini, M. (2023). Seawater intrusion assessment along the Volturno River (Italy) via numerical modeling and spectral analysis. *Journal of Hydrology*, *626*(October). https://doi.org/10.1016/j.jhydrol.2023.130289

Gong, W., Shen, J., & Jia, L. (2013). Salt intrusion during the dry season in the Huangmaohai Estuary, Pearl River Delta, China. *Journal of Marine Systems*, *111–112*, 235–252. https://doi.org/https://doi.org/10.1016/j.jmarsys.2012.11.006

Grismer, M. E., & Bali, K. M. (2015). Drought Tip: Use of Saline Drain Water for Crop Production. *Drought Tip: Use of Saline Drain Water for Crop Production*, *October*. https://doi.org/10.3733/ucanr.8554

Haddout, S., Maslouhi, A., & Magrane, B. (2018). A 2D fluid motion model of the estuarine water circulation: Physical analysis of the salinity stratification in the Sebou estuary. *The European Physical Journal Plus*, *133*(2), 79. https://doi.org/10.1140/epjp/i2018-11890-6

Haque, A., Hossain, K. M. A., & Shadia, N. (2021). Coupled 1D Hydrodynamic-Water Quality Model of Kobadak-Sibsa River System for Salinity. *International Journal of Environmental Science and Development*, *12*(10), 311–315.

Hebert, D. L. (2019). Intrusions. *Encyclopedia of Ocean Sciences*, 555–559. https://doi.org/10.1016/B978-0-12-813081-0.00148-8

Hien, N. T., Ranzi, R., & Cat, V. M. (2018). Potential Use of Reservoirs for Mitigating Saline Intrusion in the Coastal Areas of Red River Delta. *Proceedings - 2018 IEEE International Conference on Environment and Electrical Engineering and 2018 IEEE Industrial and Commercial Power Systems Europe, EEEIC/I and CPS Europe 2018*, *November*. https://doi.org/10.1109/EEEIC.2018.8493799

Hien, N. T., Yen, N. H., Balistrocchi, M., Peli, M., Cat, V. M., & Ranzi, R. (2023). Salinity dynamics under different water management plans coupled with sea level rise scenarios in the Red River Delta, Vietnam. *Journal of Hydro-Environment Research*, *51*(October), 67–81. https://doi.org/10.1016/j.jher.2023.10.003

Hong, B., Liu, Z., Shen, J., Wu, H., Gong, W., Xu, H., & Wang, D. (2020). Potential physical impacts of sea-level rise on the Pearl River Estuary, China. *Journal of Marine Systems*, *201*, 103245. https://doi.org/https://doi.org/10.1016/j.jmarsys.2019.103245

Jeong, S., Yeon, K., Hur, Y., & Oh, K. (2010). Salinity intrusion characteristics analysis using EFDC model in the downstream of Geum River. *Journal of Environmental Sciences*, *22*(6), 934–939. https://doi.org/10.1016/S1001-0742(09)60201-1

Kaddi, Y., Cierco, F. X., Faure, J. B., & Proust, S. (2022). New Developments in a 1D+ ISM Model for Operational Purposes. In *Springer Water*. Springer Nature Singapore. https://doi.org/10.1007/978-981-19-1600-7_5

Khong, T. D., Young, M. D., Loch, A., & Thennakoon, J. (2018). Mekong River Delta farm-household willingness to pay for salinity intrusion risk reduction. *Agricultural Water Management*, *200*, 80–89. https://doi.org/https://doi.org/10.1016/j.agwat.2017.12.010

Kotuby-Amacher, J., Koenig, R., & Kitchen, B. (2000). Salinity and Plant Tolerance. *UtahStateUniversity*, *January 2000*, 1–8.

Lafta, A. A. (2022). Numerical assessment of Karun river influence on salinity intrusion in the Shatt Al-Arab river estuary, northwest of Arabian Gulf. *Applied Water Science*, *12*(6), 124. https://doi.org/10.1007/s13201-022-01640-4

Lee, H. L., Tangang, F., Hamid, M. R., Benson, Y., & Razali, M. R. (2016). Modeling the Influence of River Flow and Salt Water Intrusion in the Terengganu Estuary, Malaysia. *IOP Conference Series: Materials Science and Engineering*, *136*(1), 12076. https://doi.org/10.1088/1757-899X/136/1/012076

Lindenschmidt, K.-E. (2006). The effect of complexity on parameter sensitivity and model uncertainty in river water quality modelling. *Ecological Modelling*, *190*(1), 72–86. https://doi.org/https://doi.org/10.1016/j.ecolmodel.2005.04.016

Liu, B., Liao, Y., Yan, S., & Yan, H. (2017). Dynamic characteristics of saltwater intrusion in the Pearl River Estuary, China. *Natural Hazards*, *89*(3), 1097–1117. https://doi.org/10.1007/s11069-017-3010-4

Liu, B., Peng, S., Liao, Y., & Wang, H. (2019). The characteristics and causes of increasingly severe saltwater intrusion in Pearl River Estuary. *Estuarine, Coastal and Shelf Science*, *220*, 54–63. https://doi.org/https://doi.org/10.1016/j.ecss.2019.02.041

Maruthai, S., Rajendran, S., Selvanarayanan, R., & Gowri, S. (2025). Wastewater recycling integration with IoT sensor vision for real-time monitoring and transforming polluted ponds into clean ponds using HG-RNN. *Global Nest Journal*, *27*(4). https://doi.org/10.30955/gnj.06758

Meisner, C. (2007). WPS4136 The Impact of Sea Level Rise on Developing Countries. *Tropical Agriculture*.

Miller, R. L. (2023). Forcing uncertainty and salinity response to dredging in a tidal freshwater river. *International Journal of River Basin Management*, *21*(2), 243–251. https://doi.org/10.1080/15715124.2021.1961795

Ministry of Natural Resources and Environment of Vietnam. (2021). *Climate Change Scenario* (2020th ed.). NARENCA.

NARBO (Network of Asian River Basin Organizations). (2006). *Flood management in the Red-Thai Binh river basin*. The 2nd General Meeting (Indonesia). https://www.narbo.jp/data/01_events/materials/gm02_2_2_05pa.pdf

Oude Essink, G. H. P. (2001). Improving fresh groundwater supply—problems and solutions. *Ocean & Coastal Management*, *44*(5), 429–449. https://doi.org/https://doi.org/10.1016/S0964-5691(01)00057-6

Perales-Valdivia, H., Sanay-González, R., & Valle-Levinson, A. (2018). Effects of tides, wind, and river discharge on the salt intrusion in a microtidal tropical estuary. *Regional Studies in Marine Science*, *24*, 400–410. https://doi.org/https://doi.org/10.1016/j.rsma.2018.10.001

Rice, K. C., Hong, B., & Shen, J. (2012). Assessment of salinity intrusion in the James and Chickahominy Rivers as a result of simulated sea-level rise in Chesapeake Bay, East Coast, USA. *Journal of Environmental Management*, *111*, 61–69. https://doi.org/10.1016/j.jenvman.2012.06.036

Shen, Y., Jia, H., Li, C., & Tang, J. (2018). Numerical simulation of saltwater intrusion and storm surge effects of reclamation in Pearl River Estuary, China. *Applied Ocean Research*, *79*(July), 101–112. https://doi.org/10.1016/j.apor.2018.07.013

Thai, T. H., & Thuc, T. (2011). Impacts of climate change on the flow in Hong-Thai Binh and Dong Nai river basins. *VNU Journal of Science, Earth Sciences*, *27*(December), 98–106.

Thanh, T. N., Huynh Van, H., Vo Minh, H., & Tri, V. P. D. (2023). Salinity Intrusion Trends under the Impacts of Upstream Discharge and Sea Level Rise along the Co Chien River and Hau River in the Vietnamese Mekong Delta. *Climate*, *11*(3). https://doi.org/10.3390/cli11030066

Tian, R. (2019). Factors controlling saltwater intrusion across multi-time scales in estuaries, Chester River, Chesapeake Bay. *Estuarine, Coastal and Shelf Science*, *223*, 61–73. https://doi.org/https://doi.org/10.1016/j.ecss.2019.04.041

Tu, V. T., Thuy, N. T., Hien, L. T. T., Lan, P. T. H., & Thao, N. H. P. (2021). *Preventing drought and saltwater intrusion by structural and non-structural solutions* (In Vietnam). Construction Publishing House, Vietnam.

UNDP Vietnam. (2016). *Vietnam Drought and Saltwater Intrusion: Transitioning from Emergency to Recovery*. *July* 17.

Veerapaga, N., Azhikodan, G., Shintani, T., Iwamoto, N., & Yokoyama, K. (2019). A three-dimensional environmental hydrodynamic model, Fantom-Refined: Validation and application for saltwater intrusion in a meso-macrotidal estuary. *Ocean Modelling*, *141*, 101425. https://doi.org/https://doi.org/10.1016/j.ocemod.2019.101425

Venkatraman, M., Surendran, R., Srinivasulu, S., & Vijayakumar, K. (2025). Water quality prediction and classification using attention based deep differential recurflownet with logistic giant armadillo optimization. *Global Nest Journal*, *27*(1), 1–13. https://doi.org/10.30955/gnj.06799

Vuong Tai, C., Nguyen Khanh, L., Vu Huong, N., Dinh Nhat, Q., & Truong Van, A. (2021). Investigation of saltwater intrusion in thach han river system by mike hydro river package. *Transport and Communications Science Journal*, *72*(1), 46–57. https://doi.org/10.47869/tcsj.72.1.6

Wang, J., Li, L., He, Z., Kalhoro, N. A., & Xu, D. (2019). Numerical modelling study of seawater intrusion in Indus River Estuary, Pakistan. *Ocean Engineering*, *184*(May), 74–84. https://doi.org/10.1016/j.oceaneng.2019.05.029

Yuan, R., Zhu, J., & Wang, B. (2015). Impact of Sea-Level Rise on Saltwater Intrusion in the Pearl River Estuary. *Journal of Coastal Research*, *31*(2), 477–487. https://doi.org/10.2112/JCOASTRES-D-13-00063.1

Zhang, W., Feng, H., Zheng, J., Hoitink, A. J. F., van der Vegt, M., Zhu, Y., & Cai, H. (2013). Numerical Simulation and Analysis of Saltwater Intrusion Lengths in the Pearl River Delta, China. *Journal of Coastal Research*, *29*(2), 372–382. https://doi.org/10.2112/JCOASTRES-D-12-00068.1

Zhang, W., Ruan, X., Zheng, J., Zhu, Y., & Wu, H. (2010). Long-term change in tidal dynamics and its cause in the Pearl River Delta, China. *Geomorphology*, *120*(3), 209–223. https://doi.org/https://doi.org/10.1016/j.geomorph.2010.03.031